Laser Ignition of Oil Spills
Engineering Design

Report no. 3016
March 31, 1986

AASS AEROSPACE

A Division of H.Aass Aero Engineering Ltd.

AASS AEROSPACE INC.

1685 Flint Road
Downsview, Ontario
M3J 2W8
TEL: (416) 736-7070

Laser Ignition of Oil Spills
Engineering Design

Report no. 3016
March 31, 1986

DSS Contract Serial no. OSS85-00166

PREPARED BY:

W.L. Kung
J. Wong
H.S.B. Scholaert

Aass Aerospace
1685 Flint Road
Downsview, Ontario
M3J 2W8
CANADA

M.B. Frish
M.A. DeFaccio
P.E. Nebolsine

Physical Sciences Inc.
Dascomb Research Park
P.O.Box 3100
Andover, MA 01810
U.S.A.

TABLE OF CONTENTS

LIST OF FIGURES

1. INTRODUCTION

1.1 Summary of Current Program

An engineering design of a prototype system for the laser ignition of oil spills (LIOS) from a hovering helicopter has been completed by AASS Aerospace in conjunction with Physical Sciences Inc. This system is intended for use in the Arctic, where a major oil spill can result in tens of thousands of small pools of oil scattered over the surface of an ice field[1]. Pyrotechnic igniters distributed from airborne vehicles have been used to clean up these spills[2]. However, these devices have shelf lives of only about five years, and maintaining a sufficient supply to clean up one major spill could require a recurrent cost of several million dollars[3]. There are also significant costs associated with transportation of these items to the spill site. Laser ignition is thus a viable alternative.

The system uses a continuous-wave (CW) carbon dioxide laser to heat a portion of the surface of an oil pool to its flashpoint temperature and simultaneously establish a thermal field within the oil capable of sustaining a nascent flame. A focussed pulse of energy from a carbon dioxide laser then creates a momentary "spark" above the oil pool to ignite a fire. This technique has been proven in both laboratory and outdoor testing.

The present system is designed to:

1. be installed in a Sikorsky S-61 or comparable helicopter without affecting airworthiness or safety;

2. incorporate a 1000 watt CW CO_2 laser for irradiating the oil with the required preheating intensity;

3. incorporate a pulsed CO_2 laser which is focussed to provide sufficient fluence to ignite fires on preheated oil pools from a distance;

4. maintain the laser beams on target despite helicopter vibration and movement;

5. provide sufficient power and cooling capability to operate all system components; and

6. be operable by aircraft maintenance technicians.

The following report details how the present design meets all of the above specifications.

1.2 Background

During the past three years, a novel dual-laser approach to starting pool fires has been developed under the sponsorship of Environment Canada. In Phase I[4] of that program, the technique was developed theoretically and laboratory tested, while Phase II[5] showed that the technique worked outdoors in conditions simulating an Arctic environment. The process may be summarized as follows: a continuous-wave (CW) CO_2 laser is used to heat a portion of the surface of an oil pool to its flashpoint temperature and simultaneously establish a thermal field within the oil which will not quench a nascent flame. A focussed, pulsed laser beam then provides sufficient energy to create a momentary "spark" above the oil surface to ignite a fire.

The technical advances that led to the success of the technique were: 1) learning the requirements to start a small diffusion flame which is able to both sustain itself and spread over a large pool of cold oil, and 2) determining how to satisfy these requirements using lasers. A schematic illustration of a one-dimensional diffusion flame is presented in Figure 1-1. At the surface of the cold liquid is a relatively hot layer from which fuel vapour evaporates and mixes with the air above. Combustion occurs in a very narrow layer located a small distance above the surface of the fuel, and combustion products, such as hot soot and gases rise above this zone. As the fire burns, combustion energy is radiated and conducted through the air back to the oil pool, thus providing the power required to continue vaporization of new fuel and sustain the burning. If this power is insufficient to overcome the heat flux transported to the bulk liquid by conduction and convection, the surface cools to a temperature below that at which sufficient vapour is produced, i.e. below the flashpoint, and the fire extinguishes itself. Thus, the liquid will burn only after several criteria are satisfied: 1) the surface of the liquid must be hot enough to provide a vapour above the surface which, when mixed with ambient air, is combustible; 2) this vapour/air mixture must be raised briefly to a temperature sufficiently high to initiate combustion; and 3) the liquid fuel must establish temperature and flow fields which transport less power into the liquid's volume than a nascent flame is capable of supplying back to the liquid surface.

Cold, aged crude oils fail to inherently satisfy any of these criteria. To generate a combustible vapour mixture, the surface of the liquid must be heated to its flashpoint temperature, typically as high as 100 °C[6]. To ignite the vapour mixture, it must be exposed to a heat source of 700 °C or more. The third criteria requires that the liquid absorb a certain amount of energy before the fire is ignited.

Laser beams, which act as remote infrared energy sources, may be used to satisfy each of these requirements. It is possible to select combinations of laser power, intensity (power/unit area), and irradiation time which enable ignition of sustained, spreading fires on the surfaces

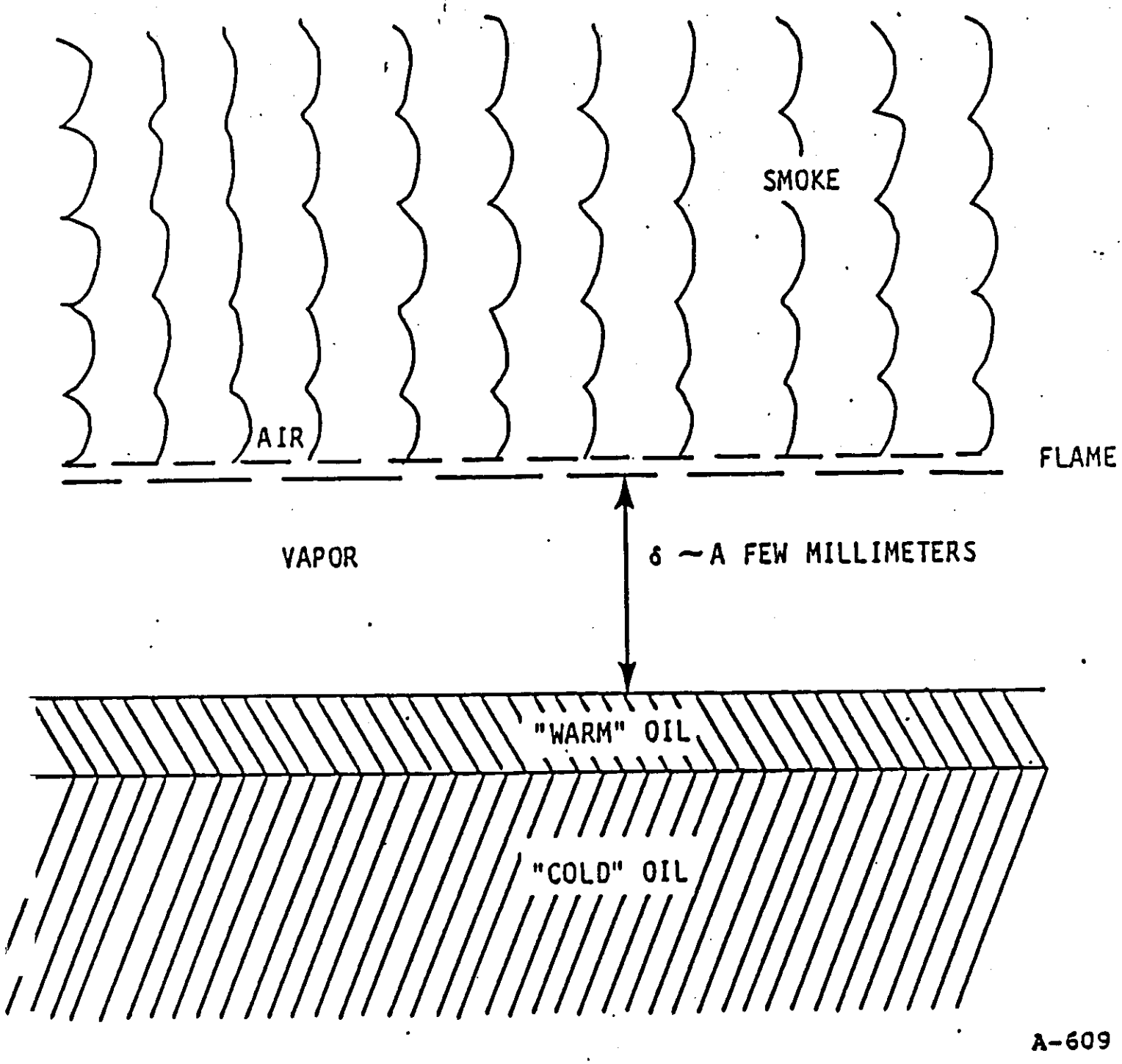

Figure 1-1. Schematic illustration of a one-dimensional diffusion flame.

of cold, aged oil pools. The power and intensity delivered by the beams are controlled by the choice of lasers and the use of focusing and defocussing optical components. By using two lasers in tandem, self-sustaining and spreading fires can be ignited as illustrated by Figure 1-2. A moderate power (<1000 W) CW laser continuously irradiates or "preheats" a small portion of the oil surface thereby establishing the thermal and flow fields required for vapour production and flame survival (satisfying criteria 1 and 3), while a high power (7 MW) short-pulsed (2 μs) focussed laser fires once per second until it ignites the vapour mixture (satisfying criterion 2). As soon as it is clear that the fire is self-sustaining, as indicated by the onset of spreading, the lasers are shut off. CO_2 lasers have been used exclusively in this technique because of their advanced state of development, energy conversion efficiency, availability and cost. These lasers radiate at a wavelength of 10.6 μm.

A pulsed laser is used as an igniter because, when focussed to high intensity in the laser-absorbing vapour above the oil, temperatures high enough to initiate the combustion reaction are achieved. It was determined in Phase I of this program that the ignition of a properly heated oil pool by a single firing of the pulsed laser requires focussing the laser beam to provide a fluence exceeding 10 J/cm² on the surface of the pool. Lower fluences yield a decreased probability of ignition on each pulse; fluences below 7 J/cm² are unusable. Since the laser used in this program supplied 15 J/pulse, focussing the beam to a spot size of roughly 1 cm in diameter was adequate to assure ignition. This was done using short focal length mirrors positioned within two meters of the oil pool.

To minimize the time required to start a self-sustaining fire, it is generally desirable to use a CW laser providing as much power as possible. Presently available lasers suitable for helicopter mounting supply up to 1000 W. In Phase II it was shown that, for the most difficult ignition scenario envisioned with a temperature of -10 °C and a 30 km/hr wind, about 30 seconds of preheating will be required to ignite each oil pool.

To utilize this technique for ignition of oil in an Arctic environment from an airborne platform, the sequence of events shown in Figure 1-3 must be followed. The sequence begins with "target acquisition": the system operator locates the position on the oil pool at which the lasers are to be aimed, points the lasers at that position, and confirms that the beams are in fact where the operator thinks they are pointed. The pulsed laser beam will be focussed by a reverse Cassegrainian telescope. The separation between the two mirrors must be selected to provide the proper effective focal length of the telescope for the distance between the helicopter and the target oil pool. After the target has been acquired and the lasers focussed, laser firing can commence, but the beams must not be allowed to drift or oscillate over such a large region as to preclude efficient heating of the oil. The system must therefore

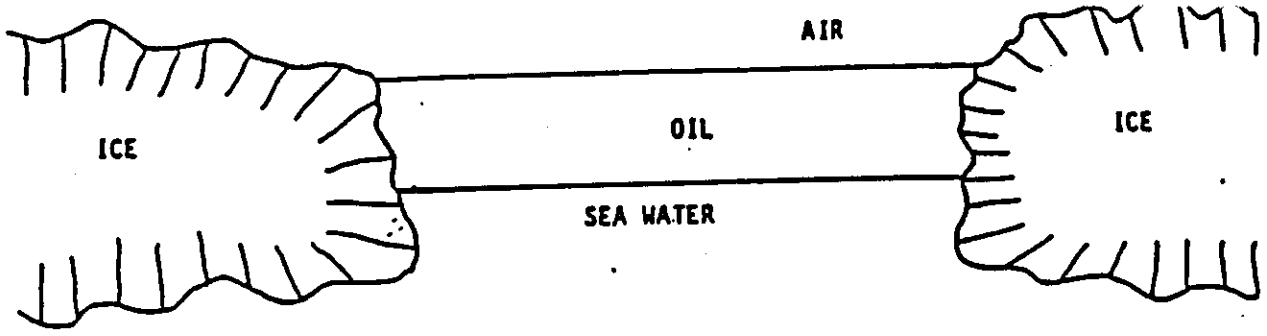

(a) A pool of cold (and therefore, unignitable) oil rests on an ice sheet

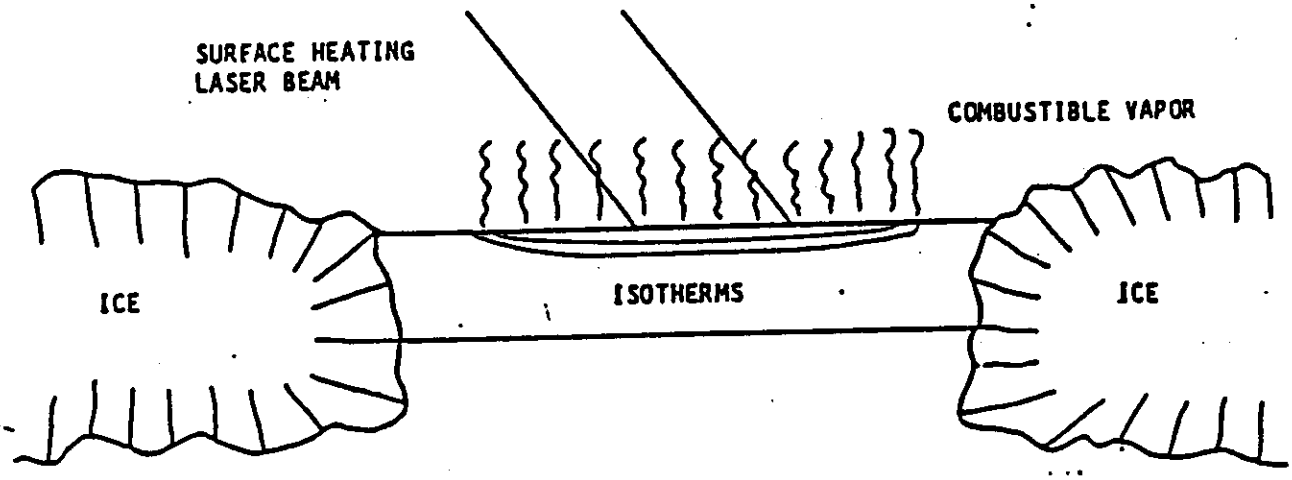

(b) A CW laser heats a surface layer of the oil pool, thus providing a combustible vapor mixture above the surface, and a thermal profile capable of sustaining combustion once ignited.

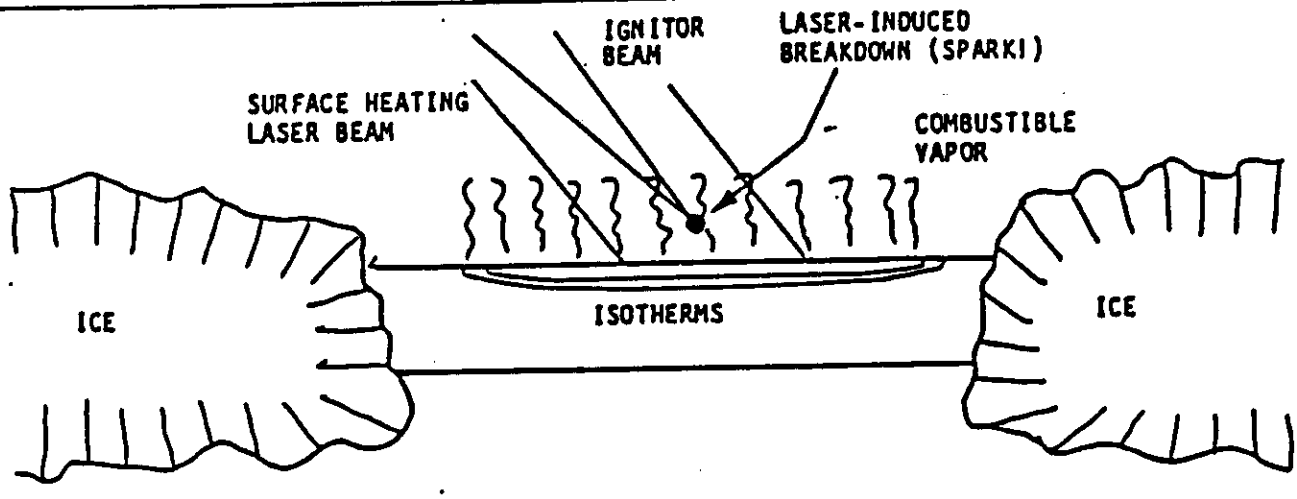

(c) A high intensity laser pulse ignites the vapor, creating a sustained, spreading flame.

A-613

Figure 1-2. Laser Ignition of Oil Spills concept and sequence.

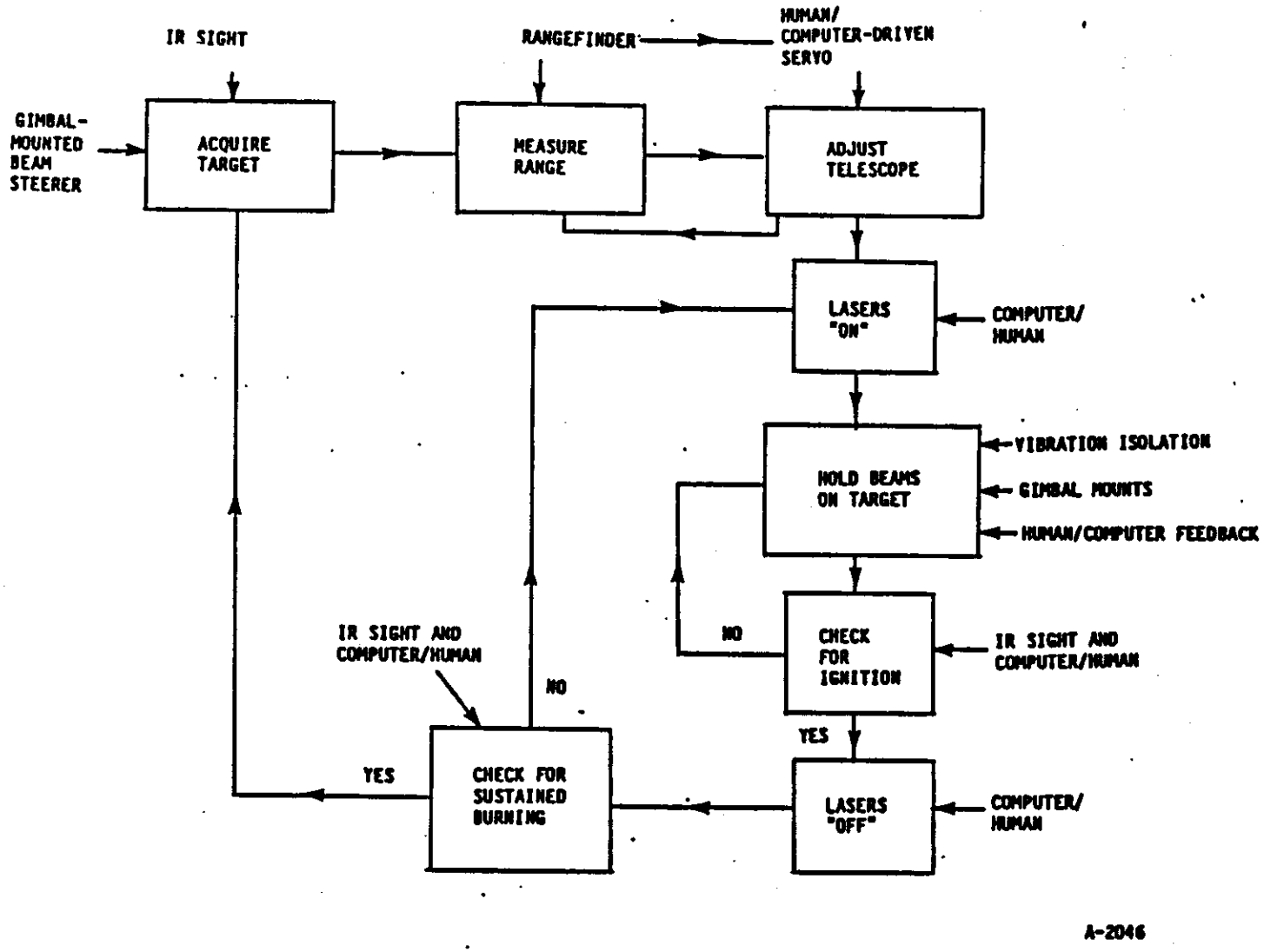

Figure 1-3. Laser ignition sequence.

be assembled to dampen the effects of high frequency helicopter vibrations and low frequency gross helicopter movements. This will require mounting the entire system on a passive vibration isolation platform to eliminate the effects of high frequency motions, and incorporating an active feedback system to compensate for slower helicopter motions. This feedback system may be human or computer controlled.

It is envisioned that both lasers will be turned on simultaneously. The CW laser will heat the oil surface, and the pulsed laser will trigger approximately once per second until a fire is ignited. When ignition occurs, the lasers can be shut off and the fire watched to ascertain its continuation. If the fire is seen to spread, then it can be assumed that the laser-supplied energy was sufficient and that the fire will continue to burn until the fuel is exhausted or thinned to the point at which the fire is quenched by thermal loss to the substrative water or ice. On the other hand, if the nascent fire is observed to diminish in size shortly after the lasers are turned off, they must be turned on again quickly to rejuvenate the fire and add more energy. Should the fire die completely, then the ignition process must be repeated. Once the fire has been determined to be self-sustaining, a new target pool can be acquired, and the entire loop repeated.

2. LASER SELECTION

2.1 CW Laser

The continuous-wave preheating laser was selected with consideration of its size, weight, ruggedness, cooling requirements, power requirements, gas consumption, ease of operation, and cost. There are two laser styles which were compared in these categories: the fast-axial-flow genre of CW CO_2 lasers of which the Coherent General EFA Series is typical, and the unique Laser Corporation of America (LCA) Falcon 800. It was found that, except for a slightly lower power and gas consumption, the EFA lasers are less suitable for the present task than the LCA device. The Falcon 800 was originally developed to be mounted on the wing of a military aircraft, and thus was designed with the small size, low weight, and ruggedness required for the present task. The total weight of the laser and control panel is just slightly under 1000 pounds. The laser head is 16 inches in diameter and 41 inches long, while the control panel measures 48x24x54 inches. A comparable EFA laser head is 102x28x23 inches and the power supply 96x51x30. The weight of this laser is unpublished, but can be presumed to be roughly proportional to the overall volume. Thus, for the highly critical size and weight considerations, the Falcon is clearly superior. Although the EFA lasers are slightly more energy efficient, they also require a lower cooling water inlet temperature (15 °C as opposed to 30 °C for the Falcon). In the recommended water cooling system (discussed later), this water, after being heated approximately 10 °C by the laser, is cooled again by passing it through a simple heat exchanger, which discharges the heat into the atmosphere. Since the efficiency of the heat exchanger increases with the difference between the air and water temperatures, it is actually easier to cool the Falcon laser because of its higher allowable water temperature. Finally, at a cost of US$80,000, the Falcon 800 is approximately 20% less expensive than the comparable Coherent General laser, although other manufacturers of fast-axial-flow lasers have published costs which are roughly equivalent to that of the Falcon.

Considering all of these factors, it is clear that, using present technology, the LCA Falcon 800 laser is the preferred laser for the LIOS system.

2.2 Pulsed Laser

In the first two phases of this program, a Lumonics Model TEA-103 pulsed TEA CO_2 laser was focussed to provide the ignition spark. This laser, operating in the multimode configuration, provided about 15 J per pulse at a repetition rate of approximately 0.5 Hz. Since preheating durations were typically several times the pulse interval, this relatively slow repetition rate did not limit the rate at which oil pools could be ignited. Experiments indicated, though, that the laser needed to be focussed to a fluence of at least 10 J/cm^2 to be certain of having an

adequate spark at this repetition rate, and somewhat lower fluences could be used if pulses were provided more frequently.

During the present design program, several recently-developed pulsed lasers were investigated to determine whether they offered any advantage over the ten-year-old Lumonics model. Characteristics including laser weight, size, beam quality, energy per pulse, repetition rate, structural integrity, power requirements, efficiency, and cost were taken into consideration. It was found that, although a whole new generation of pulsed TEA lasers has been developed (primarily for the laser marking industry), none of them offers any advantages over the pioneering Lumonics model. These new lasers, including Lumonics own TEA-800 series, operate at relatively high repetition rates, typically 5-10 Hz, but much lower pulse energies, 3-4 J. Since the higher pulse rates offer little advantage in this application, but the lower pulse energy forces the beam to be more narrowly focussed and increases the difficulty of that task, these lasers were considered to be inappropriate. Several manufacturers, including Lumonics, Pulsed Systems Inc., and Questek suggested optically coupling two individual lasers, thereby doubling the energy per pulse while maintaining a high repetition rate. However, the cost of such a customized system would be greater than the Lumonics TEA-103, which is a highly reliable, commercially available device. Since for this use little real performance increase would be realized from the added cost, this tandem laser option was also discarded. One laser, the Laser Applications Ltd. (of Great Britain) Model LT-610, is able to provide 12 J pulses at 10 Hz. This device, however, weighs and costs twice as much as the Lumonics laser, and offers no real practical advantage. The Lumonics Model TEA-103 laser is therefore the preferred pulsed laser. It is manufactured in Canada, and costs US$31,000 complete.

3. COOLING APPARATUS

The Falcon 800 laser consumes 21 kW of electricity to supply 1 kW of laser power. As much as 20 kW of heat must therefore be rejected to the external environment. The laser is water cooled. In the helicopter there can be no external supply of water, so the water must be cooled, either by transferring the heat to the air through a heat exchanger (with or without a coupled refrigeration unit), or by heating some sort of cold reservoir such as a container filled with liquid nitrogen or dry ice. Some combination of the two techniques could also be considered since the laser is not expected to be operated continuously. For example, assuming the laser is operated 25% of the time, a water cooling system which is capable of dissipating 25% of the laser power combined with a water reservoir to absorb the remaining heat during the operational period would be adequate.

Rather than explore all the various alternatives, it was decided to determine first whether the simplest solution, namely to use a commercially manufactured heat exchanger to cool a continuously operated laser, is in fact practical. The laser requires a water flow rate of 30 liters/minute with a maximum inlet temperature of 30 °C. After absorbing 20 kW, the water exits the laser at 40 °C. Thus, the heat exchanger must be able to cool water flowing at 30 l/m from 40 °C to 30 °C. This is, of course, possible without refrigeration only if the heat exchanger is supplied with ambient air at a temperature below 30 °C. In the Arctic, it is safe to assume that the ambient air temperature will be 0-5 °C. If this air is supplied to three Lytron Inc. Model 6321G3 heat exchangers, the water will be adequately cooled. These units occupy 22x12x6 inches each, including integral fans, weigh approximately 29 lbs each, and cost US$422 each. The volume and weight of each of these units is less than the corresponding amount of water which would need to be carried in a reservoir used with a lower cooling capacity and intermittent heat load. Thus, as long as the air remains cold, it is economically advantageous to provide sufficient cooling capacity to operate the laser continuously, and this approach is recommended.

The Lytron units described above are the recommended heat exchangers.

4. LASER OPTICS

4.1 CW Laser Optics

Previous work has shown that, when incident upon the oil surface, the CW laser beam should describe a circle having a diameter between about 6 and 12 cm, or an area between 28 and 115 cm^2. When incident at an angle and therefore describing an ellipse at the surface of the oil, this constraint on beam area remains valid. Ideally, the beam size which results from the natural beam divergence as it propagates to the oil pool would satisfy this constraint without additional optical components. The area of the ellipse so formed is given by

$$A = \frac{\pi}{8}\left(\frac{h\Theta}{\cos\Phi}\right)^2 \left(1 + \frac{1}{\cos\Phi}\right) \qquad (1)$$

where h is the hover altitude, Φ is the is the angle between the direction of beam propagation and the vertical, and Θ is the beam divergence. This equation, along with the constraints on irradiated area, can be used to calculate, as a function of hover altitude and laser parameters, the maximum and minimum allowable angles of incidence, ranges to the oil pool, and areas which can be ignited from a fixed position.

For example, the Falcon 800 beam emerges from the laser head with a diameter of 32 mm and has a far field divergence of 1.5 mrad full angle. If used without additional focussing or defocussing optics, the curves shown in Figure 4-1 result. They indicate that, to maximize the area that can be covered, it is desirable to hover at 40 m and aim over elevation angles ranging from straight down to 49°. The corresponding slant ranges are 40-61 m, and an area of 6,650 m^2 can be covered, assuming the helicopter is free to rotate. However, by passing the laser beam through a 12.5 m focal length lens positioned 1.2 m beyond the laser output window, the far field divergence can be halved (giving the minimum divergence that can be achieved by a single lens located at that position), thereby doubling the optimum hover altitude and quadrupling the coverage area. Although this would optimize the use of the helicopter, the maximum range at which the pulsed laser would need to be focussed, 122 m, would require exceedingly large diameter and expensive optical components. The economics of prototype construction are considered next.

4.2 Pulsed Laser Focussing

4.2.1 Economics

Assuring that the pulsed beam is focussed at the surface of the oil pool to a fluence which is sufficient to ignite the preheated oil is the most critical optical task in this program. As already mentioned, when using pulses repeating once every two seconds, the fluence per pulse must

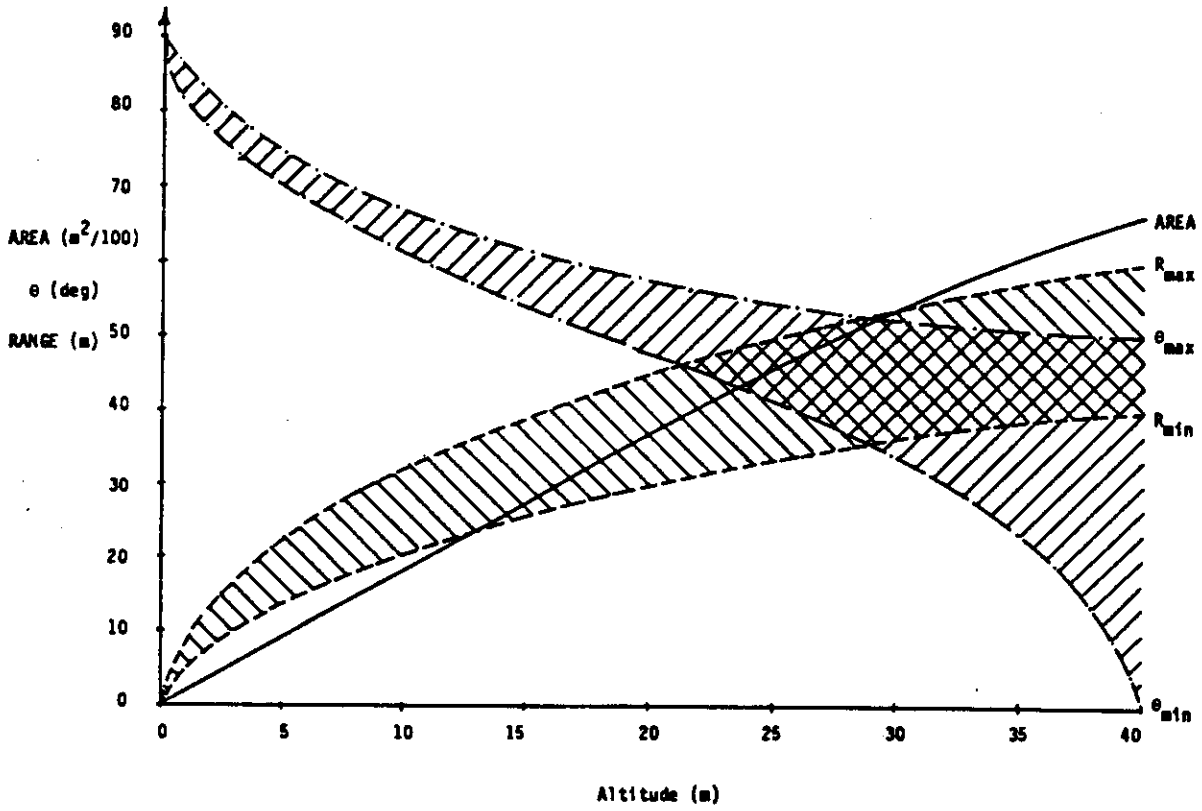

Figure 4-1. Spread of usable angles, slant ranges, and ground area covered as a function of hovering altitude using the natural divergence of the Falcon 800 laser.

exceed 10 J/cm² at the oil pool surface. Since the system will operate with the helicopter hovering at a fixed altitude of not less than 20 m above the surface, and individual oil pools selected by pointing the lasers to the extent possible rather than taxiing the helicopter, the pulsed laser focussing system must incorporate a capability to alter its effective focal length, and to determine when it is properly focussed. Because the overall cost of the focussing system was a major factor in its design, and the cost of optical elements is roughly proportional to the square of their diameter, it was clearly desirable to choose the smallest size optics, and the minimum number of optical elements suitable for the task.

The radius of the laser beam at its focal point scales as

$$r \sim \lambda R/d \qquad (2)$$

where λ is the laser wavelength (10.6 μm), R is the range to the focal point, and d is the diameter of the beam at the last focussing element. Since r cannot be allowed to exceed that value which gives the minimum allowable laser fluence ($r_{max} = \sqrt{E/\pi F_{min}}$, where E is the laser energy per pulse and F_{min} the minimum fluence), it follows that the diameter of the focussing element is minimized by minimizing the focal distance. Thus, to minimize construction costs, it is desirable to design the optical system to operate at the minimum acceptable hovering altitude of 20 m.

Referring back to Figure 4-1, the CW laser can properly preheat the oil pool from this altitude without additional optics only be aiming the lasers at elevation angles of 48-63°, with corresponding slant ranges of 31-46 m. However, if the divergence of the CW laser beam is increased by passing it through a -20 m focal length lens then, from a 20 m hover, the allowable elevation angles become 0-49°, the coverage area is 1,660 m², and slant ranges fall between 20 and 30 m. The pulsed laser focussing telescope should be designed to cover the same slant ranges.

This approach will give the lowest prototype construction costs, and is therefore recommended. Even though an additional optic to defocus the CW beam is required, a small (1.5" diameter) Zinc Selenide lens would be adequate and its cost is more than compensated by the savings incurred by the use of smaller optics for the pulsed beam. It should be emphasized that more costly systems, using larger optics but allowing a higher hover altitude and thereby providing greater ground coverage from a fixed hover are also possible, and can be designed using the same formalism discussed below.

4.2.2 Laser Operation

The Lumonics laser, operating in its multimode configuration, is nominally capable of providing 15 J per pulse. To achieve a fluence of 10 J/cm² at a range of 30 m and an angle of incidence of 49°, the beam

must be focussed to a diameter of less than 1.07 cm. Because, as is discussed later, it is not possible to measure precisely the range to the oil pool, it is necessary to actually focus the beam to a somewhat smaller diameter, thereby giving a range of distances, the so-called depth of field, over which the fluence will be sufficiently high to assure ignition. If the maximum beam diameter is selected to be 0.5 cm, then the depth of field is 3.2 m. (The system should, of course, be constructed to assure that the beam is always focussed below the oil pool, to prevent air breakdown and absorption of laser energy at the focal point. By configuring the system to intercept the oil pool at a distance of 1.6 m before the beam waist, a focussing error of ±1.6 m could be tolerated.) In the multimode configuration, the beam diameter at focus, d_3, is

$$d_3 = \Theta R d_1 / d_2 \qquad (3)$$

where d_1 and d_2 are the beam diameters at the laser output and the focussing element respectively, and Θ is the divergence of the laser beam as it emerges from the laser. This equation allows calculation of the minimum focussing element diameter. Using typical values of R=30 m, d_3=0.5 cm, d_1=3 cm, and Θ=5 mrad yields d_2=90 cm! Such a large optical element is clearly impractical for use in the LIOS system. Even if the depth of field is reduced to zero by allowing the beam waist to double in size, a 45 cm diameter mirror would be required, which is still excessively large.

This unfortunate situation can be alleviated by operating the laser in an unstable resonator configuration which, though it reduces the focussable laser power to 8 J per pulse, also reduces the nominal divergence to only 0.8 mrad. To compensate for the lower pulse energy, the beam must be focussed to a diameter of $0.5\times(8/15)^{\frac{1}{2}}$=0.37 cm, giving a minimum final optic diameter of approximately 20 cm, a much more tractable size. With this beam diameter, half the depth of field is 87 cm.

With it decided that the pulsed laser will operate in the unstable mode, a more precise calculation of the optical elements required for focussing can be performed. Assume that the focussing will be performed by a two element system such as that shown in Figure 4-2. The laser is expanded by the concave lens (lens 1), and focussed by the larger convex lens (lens 2). The distance from the focussing lens at which the beam achieves its minimum diameter can be altered by changing the separation between the two lenses, and is calculated as follows: The beam emerging from lens 1 diverges as if it were focussed at a distance f_1 to the left of the lens, where $-f_1$ is the focal length of lens 1. Thus, lens 2 receives a beam which effectively propagates from a point source located a distance

$$s_{o2} = s + f_1 \qquad (4)$$

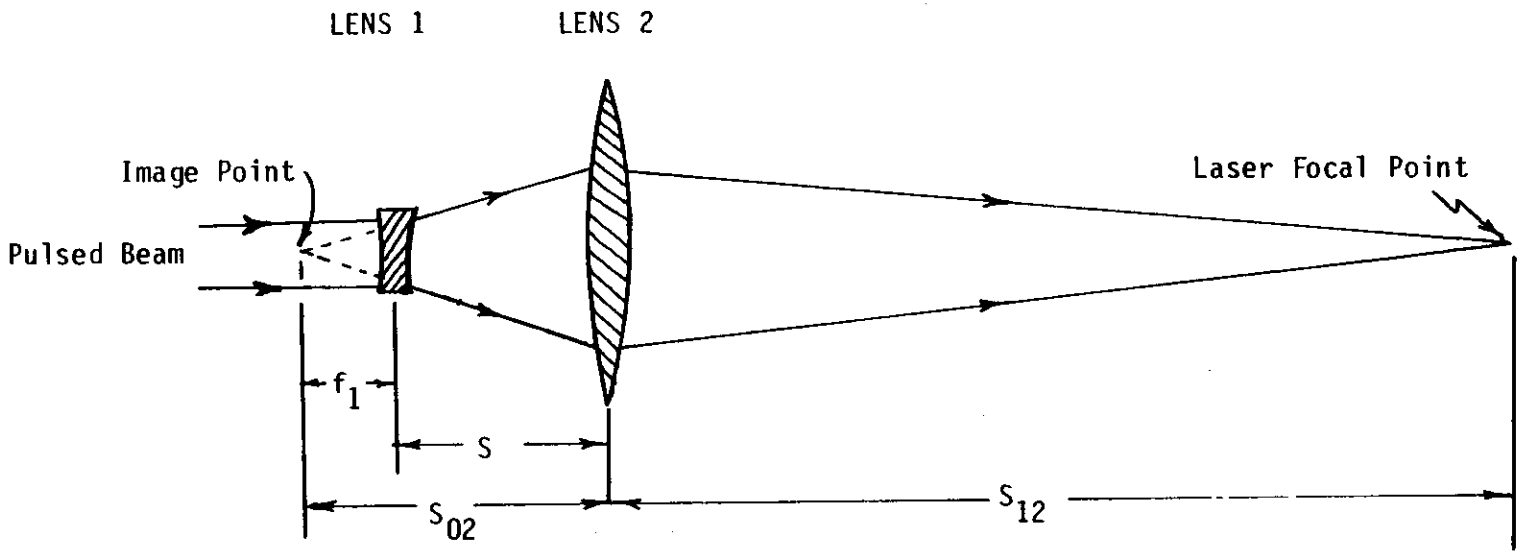

Figure 4-2. Defining sketch of two-element laser telescope.

to its left, and images that point at a distance

$$s_{i2} = s_{o2}f_2/(s_{o2}-f_2) \qquad (5)$$

to its right, where f_2 is the focal length of lens 2. Now, it is desired to vary s_{i2} within the range of 20 to 30 m by moving lens 2 and changing s_{o2} by, say, a maximum of 10 cm. This constrains f_2 to a maximum value of 2.2 m; smaller values of f_2 yield smaller relative changes in separation between lenses to cover the desired range of focal lengths.

Since the beam diameter at the oil pool must be less than 0.37 cm, its effective diameter at its image point s_{o2} to the left of lens 2 must be less than $0.37(s_{o2}/s_{i2})$ cm. The law of diffraction says that the diameter of the central spot of the focussed unstable resonator beam is given, to a good approximation, by $2.44\ f_1/d_1$. Assuming f_2=220 cm, f_1 is constrained to an absolute value of less than 33 cm. Using f_1=-33 cm, and d_1=3 cm, then geometrical optics dictates that, as expected, the beam diameter at lens 2 is 20 cm, or about 8 inches. Therefore the final focussing element should be greater than 8 inches in diameter. A rather inexpensive optic suitable for this task is a 10" diameter, 60" (152.4 cm) focal length, gold-coated parabolic mirror, available from Edmund Scientific, which can be combined with a -9" (-22.86 cm) focal length diverging lens (or mirror) to form the complete telescope. The separation between the two elements should range from 1.377 to 1.421 m to vary the effective focal length from 30 to 20 m. The position of the movable parabolic mirror relative to its position when s_{i2}=30 m is plotted in Figure 4-3.

4.2.3 Focussing and Component Layout

The accuracy with which the two optical elements must be separated is determined by the depth of field of the focussed beam, which is about 87 cm. Since over the 20-30 m focussing range the relative separation changes by 4.5 cm, the elements must be positioned with an accuracy of ±3.9 mm. The proper position can be determined and controlled by either of two methods: A) observe an image of the oil pool at position s_{o2} to the left of lens 2, and vary s until the image is in focus; or B) measure directly the distance between the telescope and the oil pool and use Eqs. (4) and (5) to calculate the appropriate separation. Option A is called passive focussing, option B is active. Although passive focussing is conceptually simpler, and probably less expensive to implement, its capability to focus the laser accurately at the proper range can be determined only by experiment. Thus, an optical layout has been designed which will allow either scheme to be employed.

The layout is illustrated in Figure 4-4. The two lasers, along with the focussing, pointing and other related optics are mounted on an integral, vibration isolated platform. All of the components, except for the lasers, are mounted on a single, rigid optical table, component #1 in

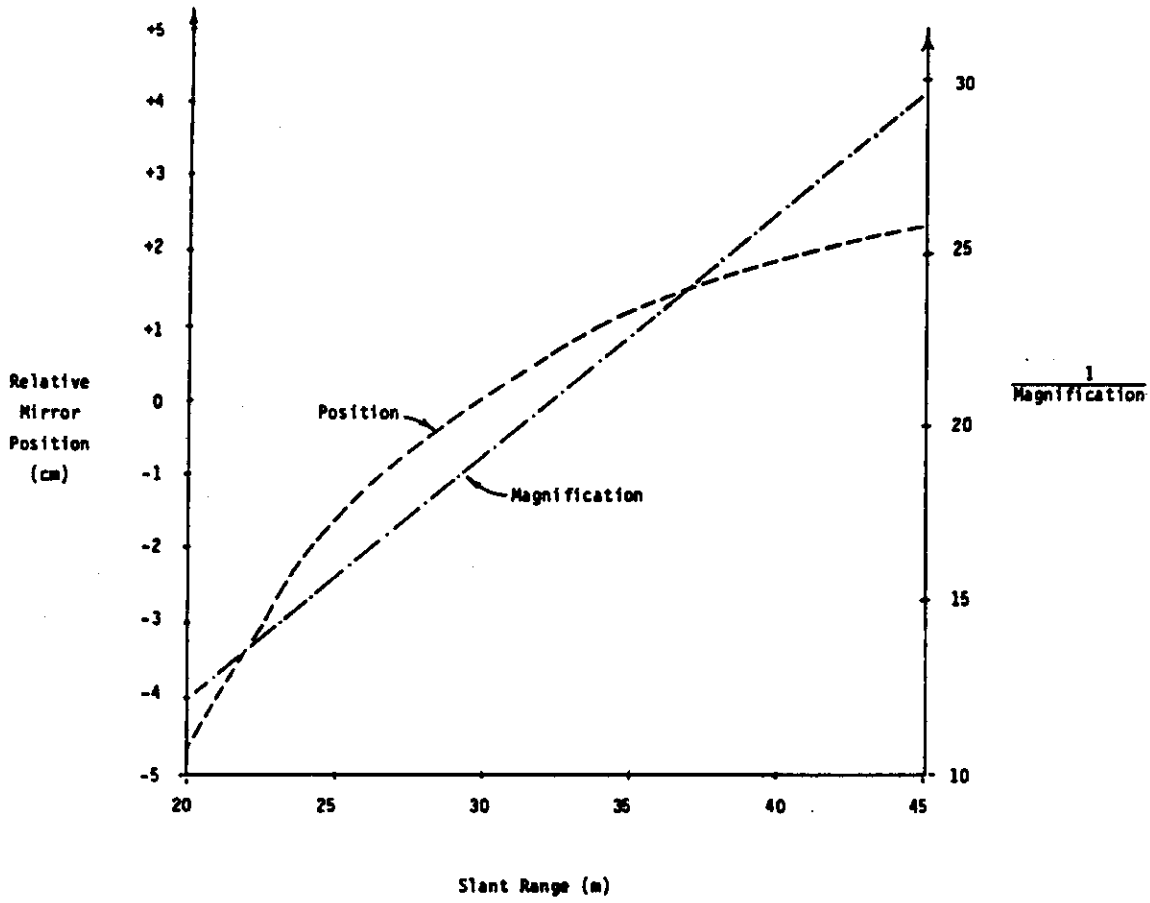

Figure 4-3. Position of focussing mirror relative to the position which focusses the pulsed laser at 30 m range, and inverse magnification of the image of the oil pool, plotted as a function of slant range to the pool.

Fig. 4-4. The lasers (components #15 and 16) lie on a shelf below the optical table, and their beams are reflected to the table surface by several small mirrors (indicated as components #9 and 10). The pulsed laser beam subsequently passes through a small hole in reflector #5 (the full function of which is discussed later), and impinges upon an anti-reflection coated, negative focal length germanium lens (component #6), which causes the beam to diverge. The diverging beam passes unaffected through a germanium flat, also coated so as to be non-reflective at the laser wavelength (component #7, discussed later), and strikes the movable focussing mirror (#11) after expanding to a diameter of about 20 cm. The slightly converging beam is reflected back along its original path, and is directed by component #5 onto the pointing mirror and subsequently onto the oil pool.

Because reflector #5 has a small hole in it to allow the pulsed beam to enter the optical system, the fraction of the expanded beam which impinges on the hole is not used in the ignition process. (Assuming that the beam is roughly uniform in intensity, this amounts to about 2% of the total energy.) However, this "hole" in the beam can be used advantageously as an area where optical elements can be mounted without additional interference with the pulsed laser beam. In particular, the relatively small diameter CW laser beam can be aligned colinearly with the pulsed beam by reflecting it from a mirror mounted within the hole, which is the function of component #8. This mirror will be held in place by three small prongs which extend from a ring having a diameter large enough so as to not interfere with the expanded pulsed beam. This configuration, which will also be used to hold components #6 and 7, will minimize energy losses to the optical holders.

This complete optical layout was designed to allow flexibility in the implementation of the focussing and pointing systems. As mentioned above, focussing of the pulsed beam can, in principle, be performed most simply by adjusting the position of mirror #11, using translation stage #12, until an image of the oil pool is brought into sharp focus at the appropriate location. Since lens 1 (component #6) causes the pulsed beam to effectively originate from a point located a distance f_1 behind the lens, and this point is imaged onto the oil pool by lens 2 (substituted by mirror #11), symmetry causes an image of the oil pool to be formed by mirror #11 and located at the effective laser origin. The image formed at this point is comprised of radiation from scattered sunlight and infrared energy emitted in response to heating by the lasers. It therefore has a fairly broad spectral distribution; it contains energy at wavelengths ranging from the visible to the far-infrared. Much of this energy can be split from the path along which the laser propagates by the germanium flat #7, which, although coated to transmit energy at 10.6 μm without reflection, is highly reflective for wavelengths shorter than about 5 μm. Thus a visible/infrared image of the oil pool is located at the image plane indicated. Since the image is formed by a single parabolic reflector, it does not suffer from spherical or chromatic

COMPONENTS

1. Optical Breadboard
2. Rangefinder (Option B)
3. IR Scanning Radiometer for Targeting System
4. Gimbal Mount for 10-12 in. Optic
5. 12 in. Diameter Gold Coated Mirror with 2 in. Hole (Option A)
   12 in. Diameter Dichroic Pyrex Window
6. -9 in. F.L., 1.5 in. Diameter AR Coated GE Lens mounted in 10 in. Diameter Ring
7. 2 in. Diameter, AR Coated (at 10.6 μm) GE Flat mounted in 14 in. Diameter Ring
8. 2 in. Gold-Coated Mirror mounted in 14 in. Diameter Ring
9. Pulsed Laser Beam Steering Mirror
10. CW Laser Beam Steering Mirror
11. 10 in. Diameter, 60 in F.L. Gold-Coated Parabolic Mirror
12. 4 in. Linear Translation Stage
13. DC Drive Motor and Electronics for Feedback Control
14. Beam Targeting System
15. CW Laser
16. Pulsed Laser
17. CW Laser Beam Diverging Lens

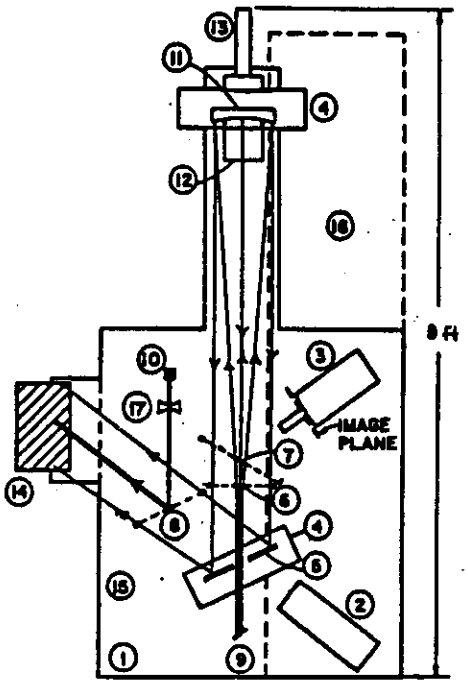

Figure 4-4. Layout of complete LIOS optical system.

aberrations, and because of the on-axis geometry, astigmatism is not a problem. The image should, therefore, be quite crisp when the system is in focus.

Using option A, this image would be all that is required to focus the telescope. A focus analyzer, for example one similar to those used in self-focussing zoom lenses, could be located at the image plane. Such a device measures the contrast at the focal plane and two planes on either side of it, and generates a voltage signal which decreases to zero when maximum contrast is located on the image plane. This voltage signal is used to drive a servo motor (component #13) which moves the imaging optic in the proper direction to optimize focussing. Although the systems used in cameras are inexpensive (the entire camera costs less than $500), no manufacturer has been found to supply the focussing system separately, and therefore a precise cost for this scheme cannot be specified. Estimates of $50,000 or more for custom manufacture of such a device have been received, which hardly seems reasonable. It is therefore recommended that, before finalizing the selection of the focussing system from the alternatives presented herein, an experiment be performed to modify a self-focussing camera for this application.

Although this focussing technique is conceptually simple, it is apparent that its accuracy (and cost) cannot be determined without experimentation. Recalling that the laser beam must be focussed to within 1 m from a distance of 30 m, the passive focussing system must be able to measure deviations of only 3%, which may be beyond its capabilities. In addition, the system requires the object to have a moderate degree of contrast. Because the cold oil pool has little contrast in itself, this requirement forces the operator to aim near the edge of the pool, where there is sharp contrast with the surrounding snow and ice. Fortunately, the magnification of the system, plotted in Figure 4-3, will allow an area approximately 35 cm in diameter to be imaged, which is roughly three times the area which must be irradiated by the CW laser. (Also, it should be recalled from Phase I that ignition near pool edges or enclosed areas is energetically favorable.)

Should experiments demonstrate that passive focussing is either inaccurate or excessively expensive, active focussing will have to be used. The active system requires a device to measure the distance to the oil pool, a lookup table or equation from which to determine the proper focussing mirror position for the measured range, and a device which sets that position. In its simplest form, which will undoubtedly be used in the first laboratory tests of the telescope, a human operator measures the range with a tape measure, calculates the appropriate mirror position, and adjusts it himself.

In the Arctic, a more sophisticated scheme is required. The most accurate means currently available for measuring distances is to use a laser rangefinder, such as the Canadian manufactured Optech Model 60. This device uses a diode laser, radiating at a wavelength of 0.9 μm (in

the near infrared), to measure distances up to 150 m with 30 cm accuracy. According to the manufacturer, it will have no difficulty measuring the distance to an oil pool even when receiving only backscattered laser radiation from a 45° angle of incidence. Thus, this device was selected as the preferred active method of measuring the range to the oil pool, should passive focussing fail. To incorporate the rangefinder into the optical system, component #5, which would be a simple gold-coated pyrex mirror for passive focussing, will be a dichroic pyrex window. It will be coated to reflect in excess of 95% of the incident CO_2 laser radiation at 10.6 μm, but transmit more than 70% of the near-IR radiation used by the rangefinder. By positioning the rangefinder as shown it can be aligned colinearly with the two lasers. The measured distance can then be fed into a computer which calculates the appropriate mirror position and drives servos to move the mirror as necessary.

The optical components for the LIOS system, along with their weights and costs, are listed in Table 1.

5. TARGETING SYSTEM

5.1 System Requirements

The output of both lasers is to be directed by a targeting mirror onto a selected oil pool. The laser beams can drift off target due to the combined effects of high frequency helicopter vibration and low frequency gross helicopter motion. The laser targeting system must compensate for the latter, keeping the laser beams on target for periods of up to 30 seconds with a centroidal drift not exceeding 2 cm. For a target range on the order of 30 m, this requirement translates into an angular deviation of 0.67 milliradians, or about 2 arc-minutes.

The basic components of the targeting system, as shown in Figure 5-1, are: a sensor that collects the target radiation and converts it to an electrical signal; signal processing electronics that process the sensor output signal to produce pointing error signals; a movable platform that permits isolation from disturbances to the pointing system and allows the sensor to compensate for helicopter motion; and a servo and stabilization system to control the platform position.

The large targeting mirror is mounted on the movable platform. Since the rotation of the laser beam about its axis of propagation is inconsequential in this application, the platform will be biaxial, consisting of an azimuth and an elevation stage, both driven by DC motors. The target should be stationary, have good optical contrast, and should be invariant with respect to rotation. These requirements are fulfilled by the thermal radiation emitted by the laser-heated oil spot. An infrared sensor that detects this radiation will be used to generate appropriate error signals to control the motion of the rotation stages.

Previous experiments[4] have shown that the oil temperature in the zone of laser irradiation exceeds 100 °C. while outside the zone the temperature is about half as high. These tests also showed that the oil takes from 1 to 2 seconds to reach its maximum temperature when irradiated with the CO_2 laser. Thus the laser-heated oil spot can provide a distinctive thermal signature for about a second, which should be ample time for the targeting system to react to shifts in the laser line-of-sight.

It is possible to incorporate a human in the targeting system, replacing the signal processing electronics. In this case the human would visually interpret the sensor output and generate suitable control signals by means of a joystick or similar device. This scheme is more economical from the viewpoint of component costs for the prototype LIOS system, since the signal processing electronics is no longer needed. However, there may still be significant costs incurred in the associated control system design. A human controller's ability to track a target is very much a function of the tracking task, helicopter dynamics, targeting system response, control system parameters and architecture. For example, it is more pleasant for the human operator to be placed in a

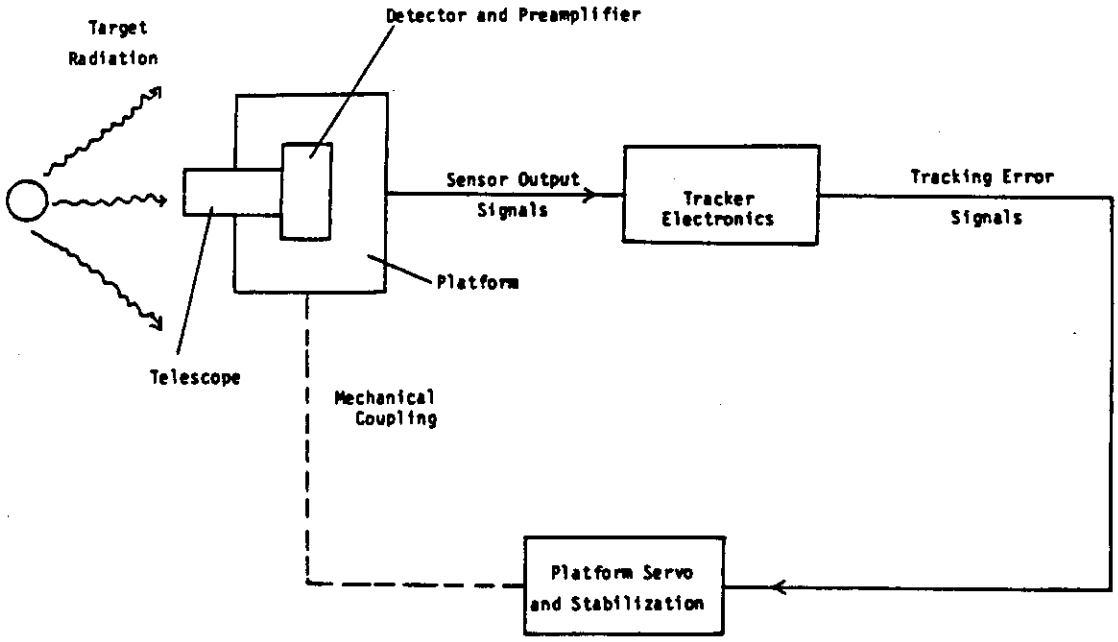

Figure 5-1. Basic components of targeting system.

position to perform pursuit rather than compensatory tracking. In the first case, the operator is given the ability to track a target with a velocity feedback input while the second case only provides position feedback. These considerations, along with the understanding that system delays also affect the requirement for some form of anticipatory control, will greatly dictate input signal parameters such as gain and sensitivity. From a systems point of view, establishing these parameters and designing or choosing an adequate control input device may prove complex and as costly as an off-the-shelf signal processing unit for automated feedback. Considering other factors such as operator training and ease of use, it is considered easier to implement a completely automated targeting system.

Manual control will be attempted with the prototype LIOS system due to its immediate cost advantage. However, the proposed tracking system is designed such that the conversion to automatic control can be easily accomplished.

5.2 Infrared Error-Sensing Schemes

5.2.1 Reticle Trackers

Three different approaches have been used to generate error signals from the output of infrared sensors[7]. These have been used primarily in infrared tracking systems, which are closely related to pointing systems. The simplest of these is the reticle tracker, which is shown schematically in Figure 5-2. In their elementary form, reticles are simple markings or fibers placed in an optical instrument to provide a convenient reference or scale. In their complex form, reticles may possess intricate geometrical patterns used to modulate or demodulate optical beams or images.

The telescope collects infrared radiation and focuses an image of the field of view upon the reticle which contains a spatial pattern of varying optical transmission. Relative motion between the image and the reticle modulates the total amount of radiation transmitted through the reticle. This radiation is focussed on the detector which produces an electrical signal proportional to the amount of incident radiant power. The electronics amplify the detector signal and demodulate it to recover an error signal which represents the location of the target within the field of view. The error signal is fed back to point the telescope so that the magnitude of the error is reduced. The zero-error target position is usually the center of the telescope's field of view.

The function of the reticle is usually twofold. The primary function is to modulate the detector signal with information indicating the target position. In addition, the reticle also performs spatial filtering, suppressing signals from large background objects relative to the signals

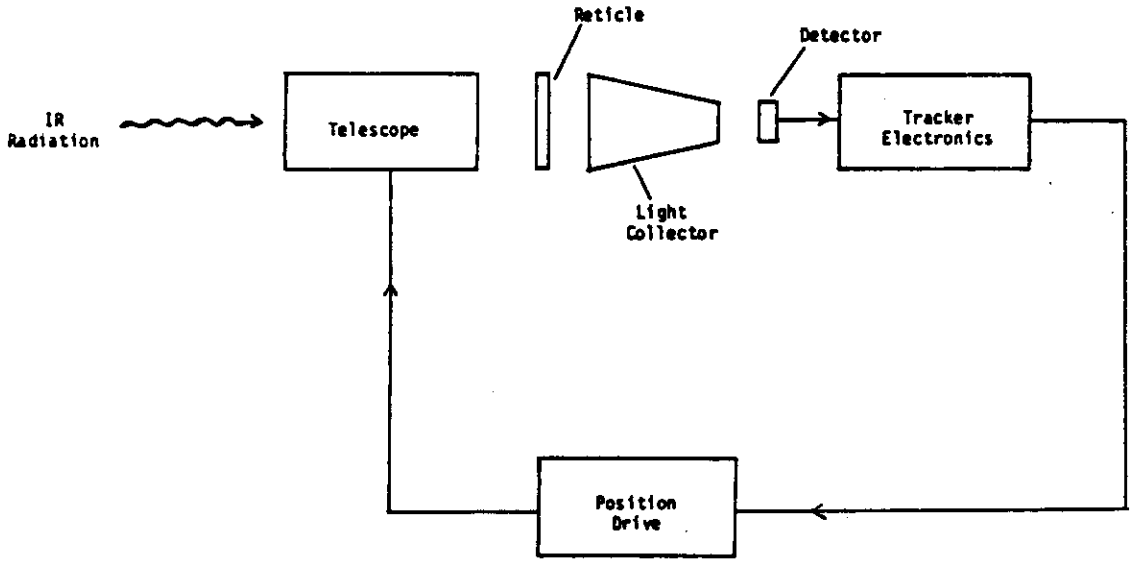

Figure 5-2. Reticle tracker.

from small target sources. Reticles function best with target sources that are small relative to the field of view.

There are many different variations possible in designing a reticle tracker. The relative motion between the image and the reticle can be provided by reticle motion, by telescope motion, or by both. Multiple reticles can be used, and there is an unlimited number of possible reticle patterns. However, it is possible to classify them according to the general technique used to encode the position of the target signal in the field of view. These techniques are amplitude modulation (AM), frequency modulation (FM), and pulse code modulation (PCM)[8]. Typical reticles for these three types are shown in Figure 5-3.

In an AM tracking system, the reticle usually rotates on the optical axis, with the center of the tracking field coincident with the center of the reticle. The position information is encoded in the form of polar coordinates. The phase of the modulation at the reticle rotation rate yields the polar angle while the signal amplitude gives the radius vector. In general, AM systems suffer from degraded performance near null due to a lack of modulation near and at the center of the reticle. In addition, the signal amplitude is a nonlinear function of the radius and is affected by target size.

The FM reticle shown in Figure 5-3(b) is used with a system that employs a conical scan. When the target is on-axis, the conical scan causes the target image to rotate symmetrically about the center of the reticle pattern, producing a constant frequency carrier signal. As the target moves off-axis, the nutating target image traces out a circular path with a center that is offset from the center of the reticle pattern. This produces a frequency modulation of the carrier at the conical scan rate. As in AM systems, the target position is encoded in the form of polar coordinates. The polar angle is given by the phase of the modulation while the radius vector is given by the magnitude of the frequency deviation.

In a PCM system, the reticle rotates about a center that is displaced by a relatively large, fixed amount from the tracker optical axis. As shown in Figure 5-3(c), the field of view is defined as a small area on the outer part of the reticle. The modulation consists of a series of pulses with variable spacing and variable timing occurring at the repetitive reticle pattern rate. Unlike the other systems, the position coding is in the form of rectangular coordinates. Pulse-pair spacing yields one axis (elevation) and pulse time of occurrence with respect to the tracker field of view gives the other axis (azimuth). PCM systems are comparable to FM systems in performance.

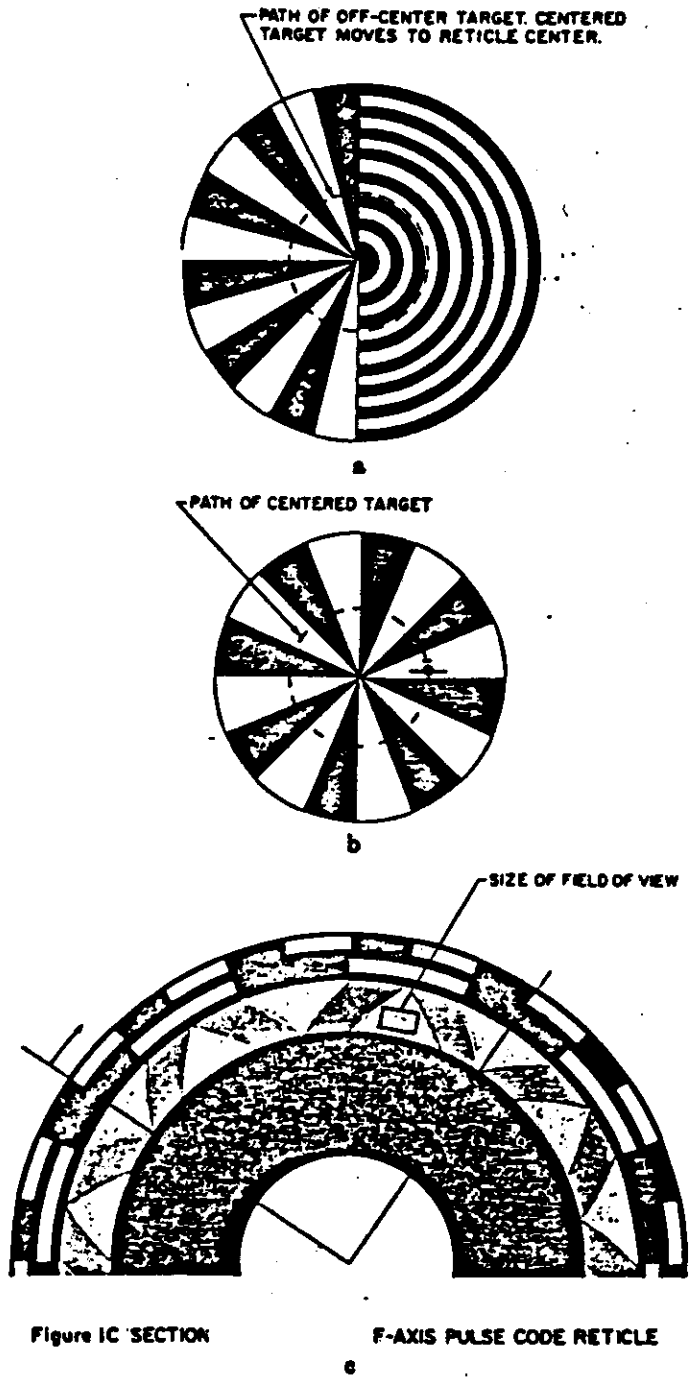

Figure 5-3. Typical reticles; (a) AM; (b) FM; (c) PCM

5.2.2 Scanning Trackers

In a scanning tracker, one or more detectors are used which have instantaneous fields of view that are small compared to the total field of view. Together, the detector fields scan the total field repeatedly, thereby transforming the scanned scene into a set of detector signals. Reference signals are generated from the scan motion that represent the instantaneous position of each detector field of view within the total field of view. When the target signal is identified in the detector signals, the reference signal is sampled simultaneously to determine the target position. These position signals are then used to place the target within the field of view.

Scanning trackers have several performance advantages over reticle trackers. Since the instantaneous field of view of each detector is smaller than that of reticle trackers, the background signals are less. Smaller detectors also mean less detector noise. More of the scene information is preserved by scanning trackers, allowing resolution of multiple targets and selection of the desired target based upon observable criteria. Extended targets can be handled by tracking a particular point on the target, such as an edge. Digital signal processing techniques can be readily implemented in scanning trackers.

An example of a scanning tracker is the basic rosette tracker, which uses a single detector with a rosette scan pattern that contains a number of loops emanating from a common center (see Figure 5-4). The scan pattern is the path traced by the projection into object space of the center of the detector's instantaneous field of view. This is done by using two counter-rotating optical elements, such as prisms, each of which deflects the incoming rays by the same angle.

Another scanning tracker uses four rectangular detectors arranged in a cross (Figure 5-5). A conical scan pattern is used, in which the image of each point in the field of view traces out a circle. The center of the circle corresponds to the location of the source point with respect to the optical axis. This type of scan is achieved by an angular displacement between the optical and mechanical axes of the telescope, combined with a rotation of the telescope about its mechanical axis.

5.2.3 Imaging Trackers

An imaging tracker uses one or more detectors which produce video signals by means of a linear raster scan of the target scene. Examples of imaging sensors are TV cameras, linearly-scanned detector arrays, and two-dimensional electronically-scanned arrays. There are basically two types of imaging trackers: gated-video trackers and correlation trackers.

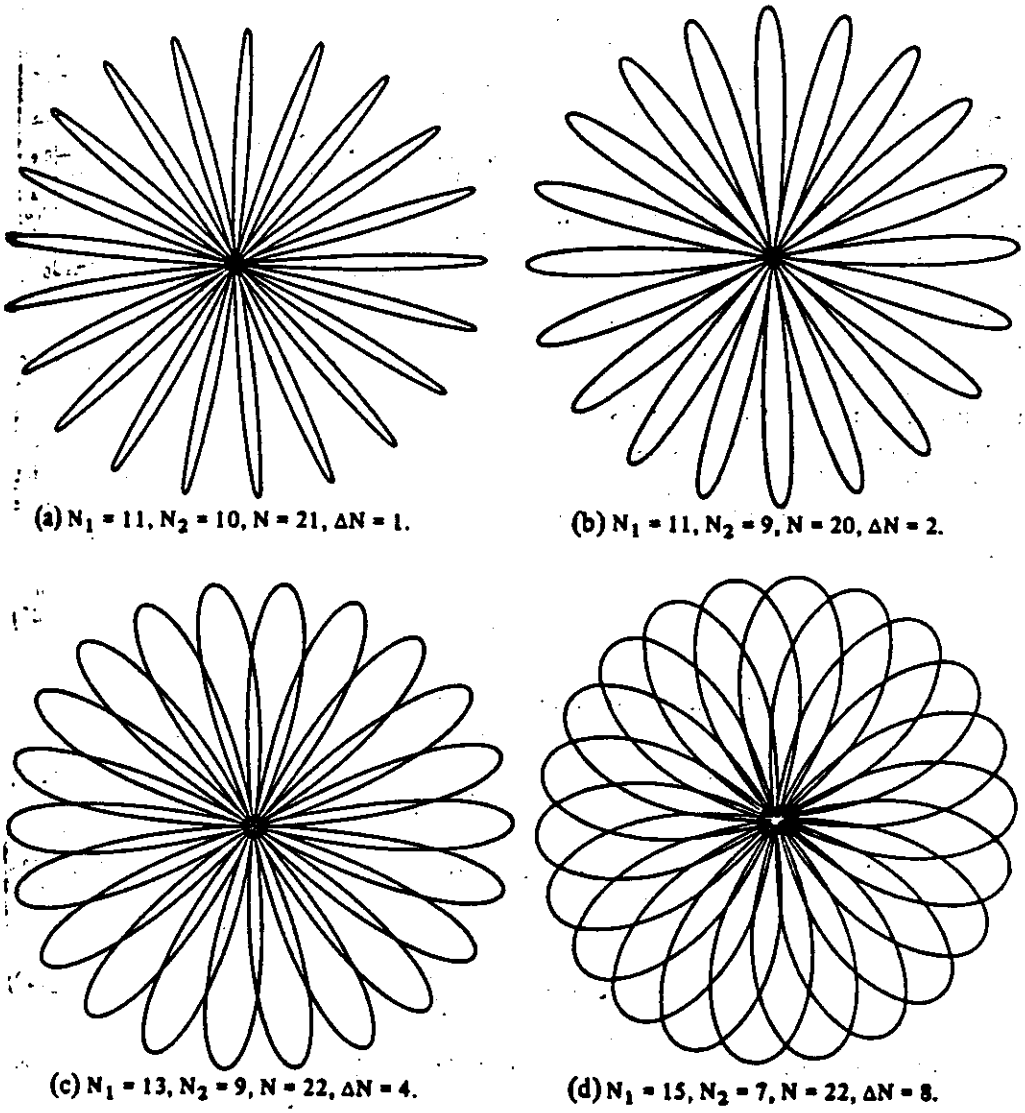

Figure 5-4. Rosette scan patterns.

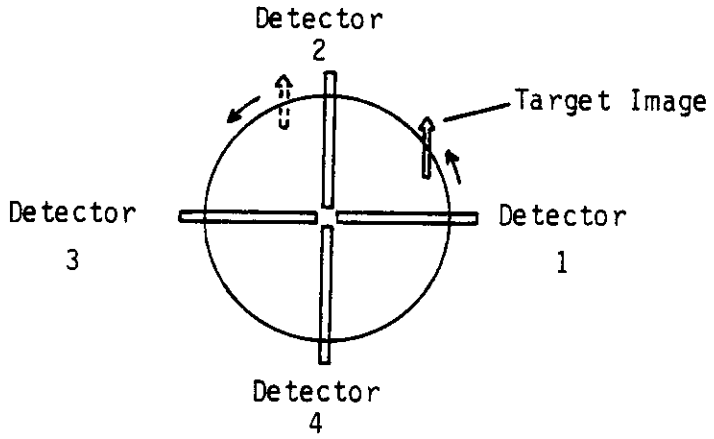

Figure 5-5. Crossed array detector.

A gated-video tracker defines some portion of the received scene to be the target image and generates tracking error signals using this information. The target-definition function is usually implemented using electronic filters, gates, and thresholding operations. For example, if the radiant intensity of the target is greater than that from the background, a thresholding operation can distinguish between them. The gate can be moved electronically, and serves to prevent scene information outside of the gated region from interfering with target tracking. Examples of target position algorithms that can generate tracking error signals with gated-video trackers are the corner-tracking algorithm and the centroid algorithm.

The corner-tracking algorithm is one of the simplest. One of the target corners, such as the leftmost point, is selected as the tracking point, and error signals are computed as a function of the position of the corner with respect to the gate center. The error signals are generated by means of the horizontal and vertical scan-reference signals, which indicate the raster point corresponding to the video signal.

In the centroid algorithm, the location of the target centroid is computed with the following equations:

$$\bar{x} = \int \frac{x\, S(x,y)\, dy\, dx}{S(x,y)\, dy\, dx}$$

$$\bar{y} = \int \frac{y\, S(x,y)\, dy\, dx}{S(x,y)\, dy\, dx}$$

where $S(x,y)$ is the target function. The error signals are generated as a function of the centroid location. The integration provided by this algorithm reduces high frequency noise, resulting in smoother tracking. The correlation tracker is the most complex to implement but offers better performance than a gated-video tracker in conditions of low contrast between target and background. In addition, a correlation tracker is preferred if the target cannot be readily identified against the background clutter. These devices determine the relative displacement between two different images of the same scene. One of the images is called the reference, and is usually taken at an earlier time. The other image, called the received image, is usually taken from the "live" scene.

The basic principle of the correlation tracker is the fact that the cross-correlation function between the received image and the reference image has a maximum at (x_o, y_o), where x_o and y_o are the respective horizontal and vertical translations between the two images. Since the direct computation of this function is very intensive and time-consuming, a number of algorithms have been devised to ease the computational requirement in practical trackers.

5.3 Pointing System Components

5.3.1 Infrared Tracker

The choice of an infrared tracking system depends on performance, cost, and availability. Reticle trackers were used extensively in the 1950's and early 60's, primarily in military applications. These systems are simple in concept and relatively easy to mechanize, resulting in low component costs compared to other infrared trackers. However, development and assembly costs would be incurred since these systems are not commercially available. In addition, better performance can be obtained with scanning or imaging tracking systems.

Scanning and imaging trackers are comparable in performance and component cost. The best imaging sensors use scanning mechanisms to generate an infrared image. However, in addition to being processed for tracking, the infrared image of the target scene can be displayed on a video monitor for initial target acquisition and performance monitoring. Both imaging sensors and video tracking processors are available commercially. On the other hand, although a number of scanning trackers have been developed, there are none available commercially. There would be a substantial investment of time and money in developing a scanning infrared sensor and the associated signal processing electronics for tracking purposes. Thus an imaging tracker is the best choice here.

The imaging tracker consists basically of the infrared sensor and the signal processing electronics. A good candidate for the former is the Inframetrics Model 525, a scanning infrared radiometer that provides a TV-compatible video output and is available for $45,000 Cdn. The AGEMA Thermovision 782 is a comparable system available at a slightly higher cost. However, its output is not TV-compatible, which is a requirement for using the video tracker described below. Thus the Inframetrics scanner is the preferred instrument for this application. This instrument will be used to sense infrared radiation in the 8-12 μm range. This range is used instead of the 3-5 μm band because the target signal is stronger and there is less interference from solar radiation in this band.

The scanning radiometer is shown as component 3 in Figure 4-4. With this arrangement, the infrared image of the oil pool is aligned with the optical axis of both lasers. Motion of the targeting mirror results in a displacement of the scanner's field of view. The anti-reflection coated Ge flat minimizes the effect of backscattered laser radiation on the infrared image.

The video signal from the infrared scanner is processed by a DBA Systems Model 606 video tracker, which has a number of features that make it useful in a tracking application. For example, it can generate and display crosshairs superimposed on the infrared video image indicating the null tracking point. One can choose between either edge or centroid

tracking modes. The tracker provides both analog and digital error signal outputs for ease of interfacing with servo components. An auxiliary video input is provided to enable one to mix externally generated signals with the composite video. A block diagram of the video tracker is given in Figure 5-6. The cost of this instrument is $45,000 Cdn.

5.3.2 Targeting Mirror and Platform

The targeting mirror is a flat, gold-coated glass mirror 24 inches in diameter and 0.75 inches thick. It is supported by a rigid mount that allows it to be attached to the movable platform. The targeting mirror platform consists of two servo-driven rotation stages that can point the mirror within a fraction of a milliradian. There are a number of U.S. companies, such as Contraves Goerz, that are capable of designing and manufacturing precision pointing platforms. Although these devices are capable of microradian pointing accuracies, their cost is high. The most cost effective method is to assemble the system using off-the-shelf components.

With this in mind, it is proposed that the platform consist of a RT 300 rotation stage and a BG 200 goniometric cradle, both from Micro-Controle. The costs of these stages are $11,000 and $12,000, respectively, in Canadian funds. The targeting mirror is mounted on the goniometric cradle, which in turn is mounted on the rotation stage. Both stages are driven by DC motors with integral tachometers and rotary encoders. The tachometers provide rate feedback to the servo controllers while the encoders indicate the angular position of the rotary stages. Limit switches are provided on both positioning stages as a safety precaution in case of control loss.

This particular mounting arrangement does not permit elevation angles near zero to be achieved. Although this limits the coverage of the LIOS system, it is not a serious drawback. An alternative arrangement could be to turn the platform upside down. However, this is a more demanding loading situation for the platform and additional costs would be incurred due to the stronger components and extra structural support required.

5.3.3 Platform Controller

The servo controller takes the output from the video tracker and adjusts the gain and compensation for the control system. The controller is implemented in a microcomputer for flexibility in control law design. The microcomputer's digital outputs are converted into analog control signals by DACs (digital to analog converters) and fed into PWM amplifiers that drive the DC motors. In addition to handling the digital output from the video tracker, the microcomputer also accepts input from the rotary encoders and from a joystick. The former allows the angular

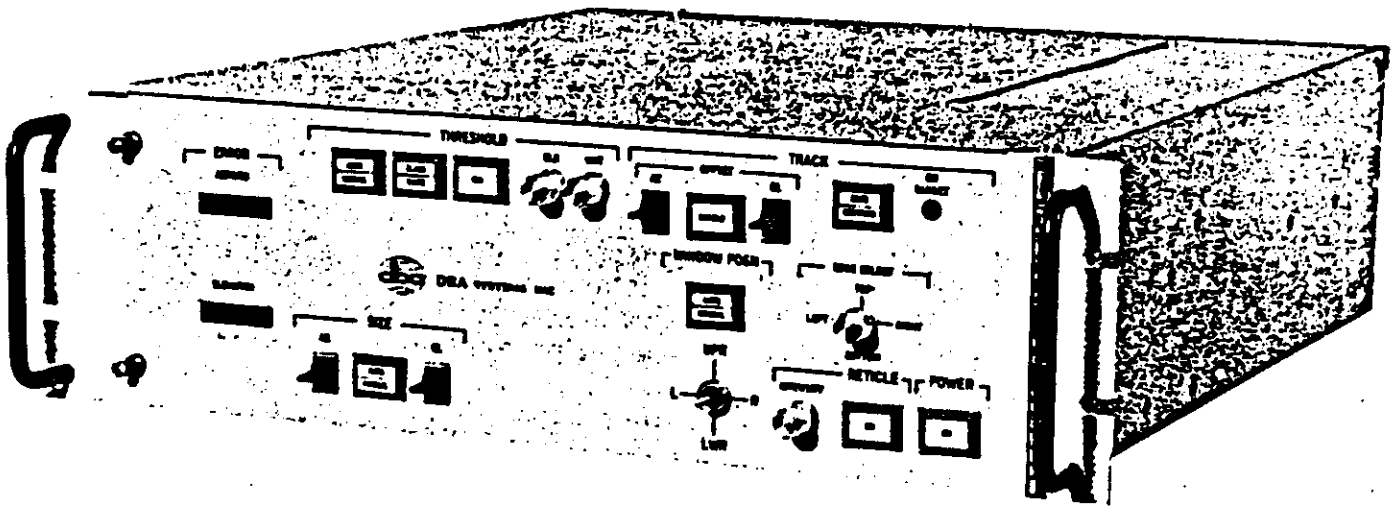

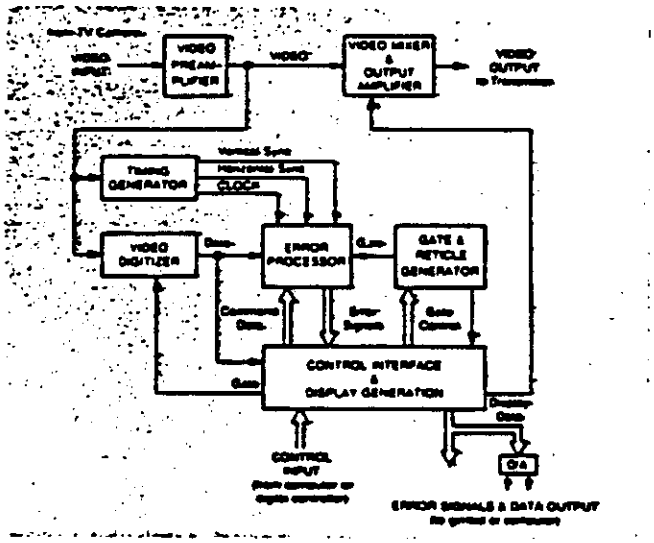

Figure 5-6. Block diagram of video tracker.

position of the rotary stages to be displayed on the screen. This information can also be used to compute the target range if the helicopter altitude is also known. The joystick permits open loop control of the targeting mirror position during the target acquisition phase. During this phase the video tracker's outputs are ignored by the microcomputer. Once the target has been acquired, the joystick is disabled and input is accepted from the video tracker, closing the control loop. A block diagram of the complete targeting system is shown in Figure 5-7. The microcomputer could also be used in the active focussing system. Costs of the various components for the targeting system are given in Table 2.

5.3.4 Target Acquisition and Tracking

The operation of the LIOS system will be based on the following sequence of events. In the target acquisition phase, the operator locates the position on the oil pool at which the lasers are to be aimed and points the lasers at that particular spot. Since there is probably very little image contrast in the infrared prior to laser heating, a video camera is used for this task. This camera can be placed near the infrared scanner, with a dichroic beam splitter directing visible wavelengths to the camera and allowing the infrared to pass through to the scanner. The camera can be connected to the video tracker, which allows the tracking crosshairs to be superimposed on the visible image of the scene. Using the joystick controls, the operator positions the targeting mirror so that a selected point on the oil pool is centered within the field of view. The optical system is adjusted to focus the lasers, which are then turned on. An infrared image of the laser-illuminated spot appears within a second and can be used for tracking purposes.

At this point, the operator can continue to hold the lasers on target with the joystick or he can switch in the video tracker for automatic tracking. Motion of the helicopter results in a displacement of the optical field of view, and hence a displacement of the infrared image of the heated spot. The time delay involved in heating and cooling the oil allows one to reposition the targeting mirror so that the hot spot is once more centered in the scene. This adjustment procedure continues until ignition of the oil is confirmed by the operator.

The LIOS system will be operated only while the helicopter is hovering to facilitate the task of keeping the laser beams on target. Using a radar altimeter for feedback, an experienced pilot can be expected to maintain a large helicopter at a desired altitude within ±1 foot for up to a minute under normal flying conditions. The helicopter motion has a low frequency, typically less than 1 Hz, and should easily be compensated by the pointing system.

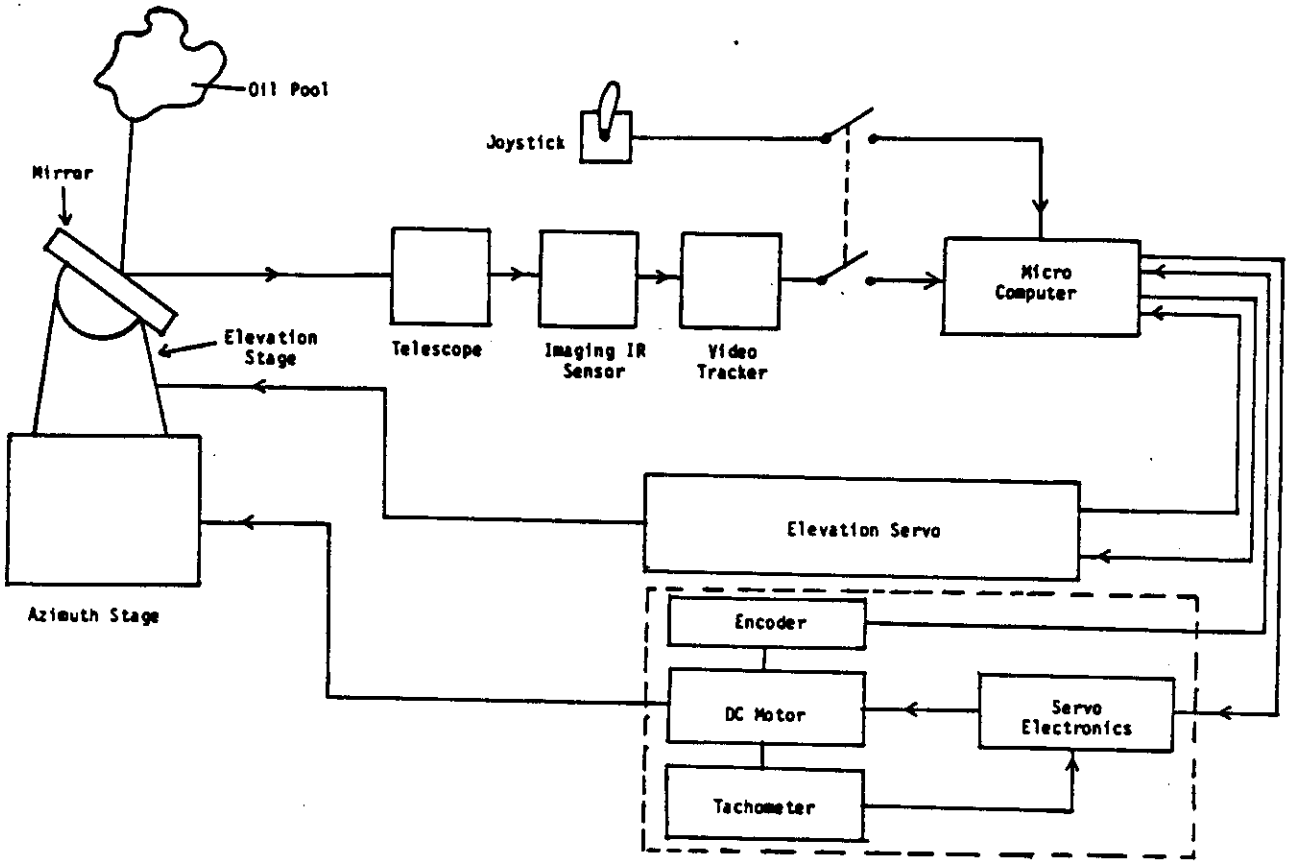

Figure 5-7. Block diagram of LIOS targeting system.

5.4 Vibration Isolation

A factor that can degrade the performance of the LIOS system is the helicopter's internal vibration, especially at the blade rotation frequency[9]. This causes jitter in the optical image, which can cause the targeting system to lose the target. Jitter is reduced by incorporating a passive vibration isolation system comprised of a number of damped springs between the optical support structure and the helicopter cabin. For example, the Sikorsky S-61 has five blades and a rotor speed of just over 3 Hz, resulting in a blade passage frequency of about 15 Hz. Thus the isolation system should be designed to have a resonant frequency below 10 Hz and to attenuate at least 90% of the vibration at 15 Hz and above. Viscoelastic-spring dampers such as the Barry H64 mounts meet these specifications although their load capability is not high. Companies such as Barry Controls and Taylor Devices have the capability to custom design an isolation system to these specifications. In addition, the optical components and support structure should be designed so that their resonant frequencies are much higher than the blade rotation frequency.

6. POWER REQUIREMENTS

The installation of the LIOS system requires the availability of a large amount of electrical power for the CW laser (21 kVA). The power requirements of all the other electrical equipment associated with the LIOS system, and the pulsed laser combined do not approach this level of power demand. In fact, the sum of the power required by all units not including the CW laser will be less than 4 kW. Using this level as a conservative upper limit, it becomes clear that this requirement can easily be satisfied by existing aircraft power supplies.

For the S-61R helicopter, there is a 300A, 28V DC generator, and two 20 kVA, 115V AC, 400 Hz generators. An existing APU is mechanically linked to the rotorcraft gearbox for use as a starter unit. Although its power output would be sufficient for the needs of this system, installation of a generator would require major modifications to the helicopter. Typical aircraft operations will require roughly 200 A DC, and approximately 28 kVA AC power. This will leave about 1 kW of DC power and 4 kW of AC power, accounting for the fact that electrical loading should not exceed 80% of the generator capacity as specified in the Canadian Department of Transport Engineering and Inspection Manual[10].

All of the electrical units will require power in the standard 120V, 60 Hz AC format, and hence, either power inverters or converters will have to be utilized. Typical efficiencies of these units are 70% for inverters (AC to DC), and somewhat less for the power converters (AC to AC) -- perhaps 50-60%. This will dictate a power availability of 7 to 8 kW. This load could well be satisfied by the aircraft power systems, if the unnecessary aircraft equipment were shut down during the operation of the LIOS system. However, the requirement of 21 kVA power for the CW laser clearly specifies that some sort of auxiliary power be available.

Installation of an Auxiliary Power Unit (APU), coupled to a suitable AC generator, can easily supply all the power requirements of the CW laser, and perhaps some of the associated electronics as well. The CW laser requires AC power with the following characteristics:

230 VAC; 3 phase; 60 Hz.

Standard aircraft APU units are available from 28 HP (21 kW) up to 150 HP (112 kW). The typical APU's, however, are in the 40 HP (30 kW) to 80 HP (60 kW) range. Assuming a generator efficiency of 75%, the 21 kVA power requirement would translate to a power capacity of 28 kVA required from the APU.

The Turbomach Division of Sundstrand manufactures a complete line of APUs for airborne systems. The cost of one large enough to meet the above power requirements is about $100,000 Cdn. A generator is necessary to convert the mechanical output of the APU into electrical power. Such

generators are available from Bendix. An alternative would be to modify a ground-based electrical power unit for mounting in the helicopter.

Installation of an APU will certainly complicate matters from the point of view of airworthiness requirements compliance; many safety measures concerning airworthiness must be satisfied, such as fire protection, a protective housing for the APU, and ventilation of the housing.

Since no APU installations of this capacity have been developed or approved under Supplemental Type Approvals (STA) in Canada or Supplemental Type Certificates in the U.S., one such installation will have to be developed for this particular system. In order to avoid major helicopter modifications, the system must be independent of aircraft fuel supply and main power bus. As such, this design must include a separate fuel system and, as indicated above, the precautions necessary to maintain airworthiness, though complex, must be implemented.

The generator, fuel tank, and fire extinguishing system are off-the-shelf items which may be acquired from a multitude of suppliers. Hardware costs associated with this equipment are estimated to be $40,000 Cdn. The APU housing, ventilation system, and refuelling system will have to be custom designed. Restrictions on the design will be dictated by the APU components chosen and helicopter cabin layout. Design and assembly of the final APU configuration, including all hardware and materials associated with the housing will add approximately $30,000 Cdn to the total cost.

7. HELICOPTER INSTALLATION

7.1 Helicopter Survey

7.1.1 Sikorsky S-61R

The primary choice of helicopter for the LIOS installation is the Sikorsky S-61, chosen for its large cabin, payload capability, and availability. Although any variant of the S-61 would satisfy the demands of this installation, the HH-3F Pelicans (S-61R) of the U.S. Coast Guard became the likely choice due to their availability at this time.

The S-61R features an approximately rectangular floor layout, with a length of 25 feet and a width of 6.5 feet. A 4 foot wide sliding door is located on the right side of the cabin, immediately behind the cockpit. The remaining exit is the large ramp cargo door in the rear of the helicopter. A possible layout of the LIOS system is shown in Figure 7-1.

7.1.2 Aerospatiale AS332 Super Puma

One of the other types of helicopters that have sufficient payload capacity for the LIOS installation is the Aerospatiale AS332 Super Puma. This helicopter is, in many aspects, similar to the S-61 series of helicopters. Cabin length of the Super Puma is 19.8 feet, and average cabin width is 5.9 feet. Although this is somewhat smaller than the 25 feet by 6.5 feet cabin of the S-61R, there should still be sufficient space in this helicopter.

Again, it must be kept in mind that the use of the LIOS system requires that an APU be available for the system. As a result, even though the cabin of the Super Puma is sufficiently large for this installation, the installation of the necessary APU will take up valuable space. The stretched version of the AS332, the AS332 L, has a cabin length of 22.3 feet, and should provide sufficient space for the LIOS installation, including the required APU. The early variants of the AS332, the B and C versions, have the shorter 19.8 feet cabin. In these helicopters, installation of the LIOS may be possible, but space will be at a premium. Extremely efficient packaging of the system is a necessity for this helicopter.

7.1.3 Bell 212/214

The civilian version of the military Twin Huey, the Bell 212, and the similar Bell 214 have sufficient payload capacity for the LIOS system, but installation is considerably hindered by the small cabin. Although this helicopter has a cabin length of 7.7 feet, and a maximum width of 8 feet, there is a housing at the back of the cabin which uses up valuable cabin space. Also, the required installation of an APU with its

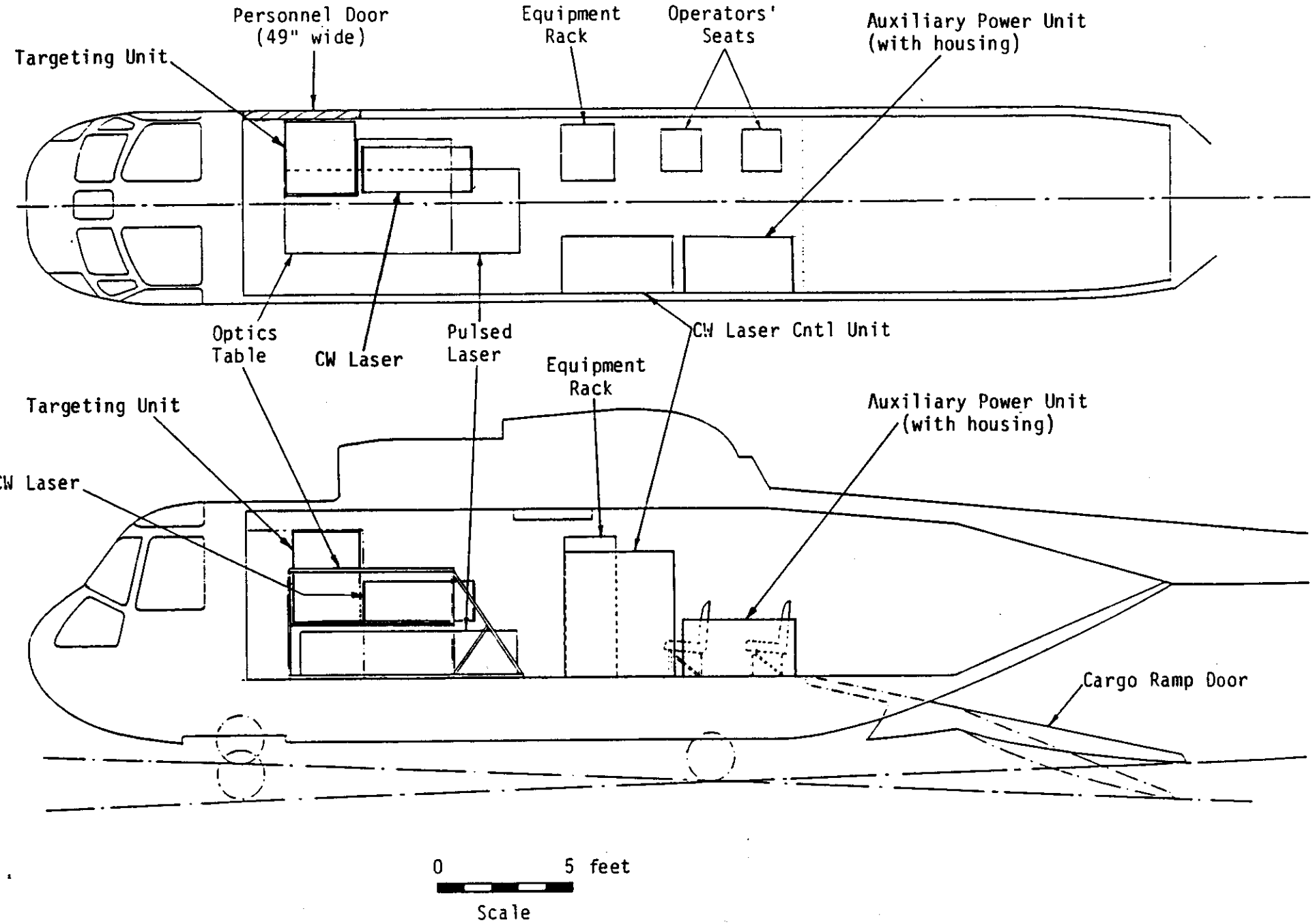

Figure 7-1. Helicopter layout of LIOS system.

associated protective structure would use up additional valuable space. With these space restrictions, these helicopters are not really suitable for installation of the LIOS system. It must be noted, that should this system decrease in size significantly in the future, consideration of this helicopter for use with the LIOS system must not be overlooked as these are the most widely available of the helicopters examined here.

7.1.4 Bell 214ST

A new variant of the Bell 214, the Bell 214ST (Super Transport), features a longer cabin length of 13.5 feet. As with the Bell 212/214 variants, an APU must be installed for the CW laser. Ideally, this helicopter will be more suited to the LIOS role than the standard 212/214 due to its larger cabin, but as with the Bell 212 and 214, a significant decrease in the LIOS system size will be required before the LIOS installation can become practical in this helicopter.

7.1.5 Other Types

Apart from the types discussed above, there is a variety of other helicopters that can be adapted for the LIOS task. The types listed above are essentially the smallest possible rotorcraft that can be used to take the LIOS system, and as a result, larger helicopters are also suitable. Although most of the ones listed in this section may provide more cabin space, or payload capability than required, they are, nevertheless, quite suitable for the task. Some of these larger helicopters include:

Aerospatiale SA321 Super Frelon
(*) Boeing Vertol CH-47 Chinook
(*) Sikorsky S-64 Skycrane
(*) Sikorsky S-65
(*) Sikorsky CH-53
Sikorsky Blackhawk

Unfortunately, the majority of these helicopters are in military use, and their availability is decidedly restricted. The capabilities of these helicopters, especially the four marked by the asterisks, represent what is probably the best in heavy-lift helicopters in the West today. As mentioned, however, with the exception of the Skycrane, most, if not all of the other types listed are operated solely in military service.

The Aerospatiale SA321 Super Frelon has an internal cargo payload capacity in excess of 11,000 lbs, and cabin dimensions of 22' by 6'2", or 31.75' by 6'5", depending on the variant. Although this helicopter is more than capable of carrying the LIOS system, its availability is decidedly limited in North America.

The CH-47 Chinook is operated both by the U.S. and Canadian armed services, and is available. Known for its heavy lift capability, the Chinook, if available for civilian use, will have little problem in supporting the LIOS system.

The Skycrane represents somewhat of a special case. Carrying the Universal Military Pod developed by Sikorsky, this pod will give a cabin space of 27.5 feet in length by 8.8 feet in width. Payload capacity of this helicopter is roughly 20,000 lbs, giving a capacity far in excess of what will be required for the LIOS system. There are variants of the Skycrane registered in the American civil aircraft registry, along with the versions used by the U.S. armed forces, and is therefore, one of the more available types of the heavy lift types listed here.

The S-65, CH-53, and HH-60 Blackhawk helicopters built by Sikorsky are in service only with the U.S. armed forces on this continent (there are overseas operators for these helicopters), and hence, access to these types are restricted.

7.2 Cabin Layout

As can be seen in Figure 7-1 above, the cabin of the S-61R is more than large enough for such an installation. The primary drawback in using this helicopter is the small width of the cabin door, as compared to a Bell 212 Twin Huey, for example. The width of 49" is marginally sufficient for the layout, but a wider door would be preferable. Installation of an APU and generator will be required to supply power to the CW laser, and the large cabin space in this helicopter allows for that installation with little difficulty.

One of the major requirements that had to be satisfied in this installation is the one of maintaining access to the available exits. With the 18" wide aisle between the laser installation and the cabin wall, this requirement is satisfied. The laser and flight crews are considered to be trained personnel, who are thoroughly familiar with the layout of the cabin, and its safety features. Although there are no emergency exits as such, the trained crews will not have any difficulty in evacuating the cabin in an emergency through the use of either the rear loading door, or the personnel door in the front of the cabin.

The cabin floor is rated for loads of 200 lb/ft^2, which is more than adequate for this installation. The optical table, focussing optics, targeting mirror and drive, lasers, and support structure weigh about 1500 lbs. A configurational drawing of this assembly is shown in Figure 7-2. This assembly will be mounted on Brownline seat tracks as will the equipment rack containing the control electronics. The loaded rack is expected to weigh about 150 to 200 lbs. For ease of integration, all equipment will be packaged prior to installation in the helicopter. Structural frames will be of welded 6061-T6 aluminum construction. The

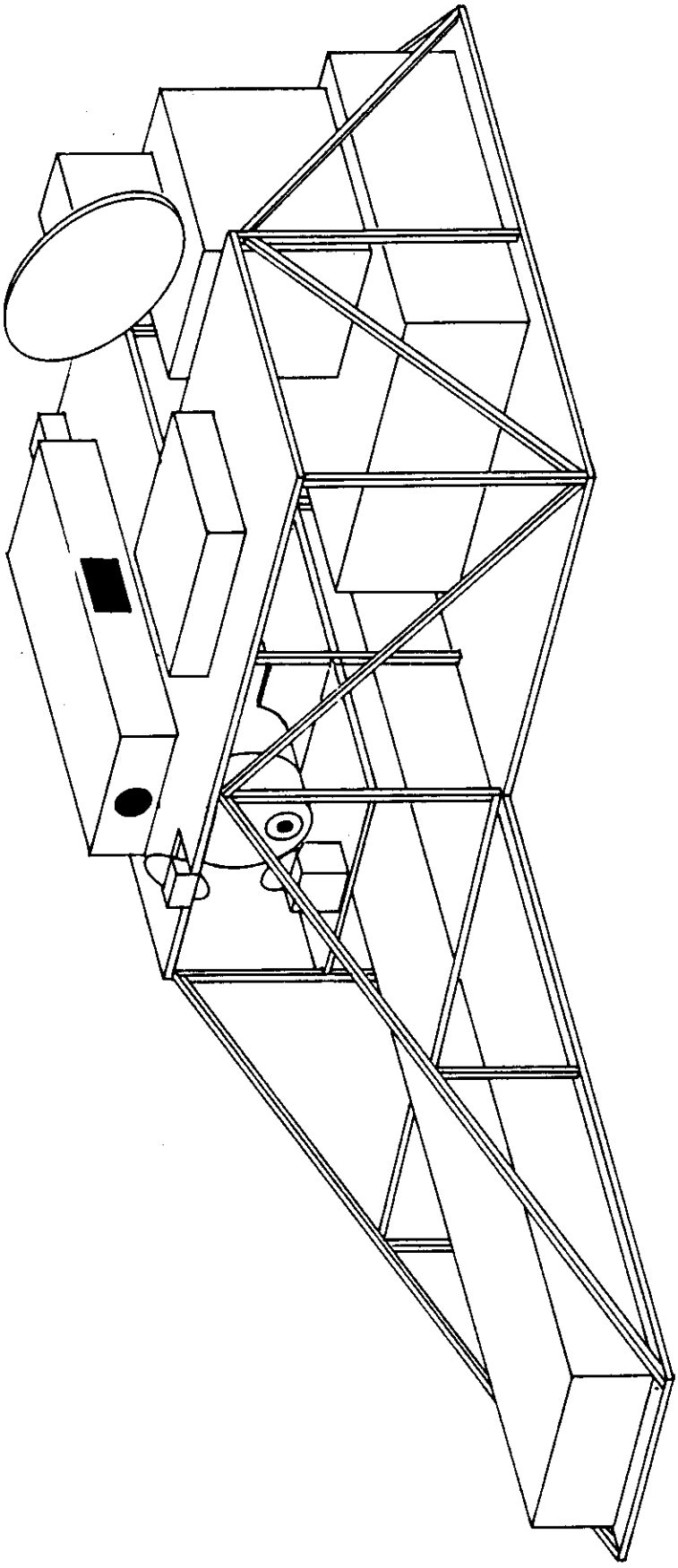

Figure 7-2. Configuration drawing of LIOS assembly.

laser consoles together weigh nearly 700 lbs and are situated to one side. The heat exchangers will be mounted on a separate rack and ducting will be provided to ensure a supply of cool air. Finally, the APU and generator will be installed with protective housings.

Material costs necessary for such an installation are not expected to exceed $1500 Cdn. The majority of expenditures will be incurred by the associated labor costs. Two men will likely require at most 5 days to fully install and integrate the system. Using standard labor rates associated with this type of work, total installation is conservatively estimated to be $3000 Cdn. Table 3 summarizes the costs for the APU and LIOS system installation.

8. CONCLUSION

A configurational engineering design for a helicopter-based dual-laser system for igniting oil spills has been completed. The system is to be operated by trained aircraft technicians while the helicopter is hovering at an altitude of 20 m. The system incorporates a Falcon 800 CW CO_2 laser for preheating the oil and a Lumonics TEA-103 pulsed CO_2 laser for ignition. The CW laser is water-cooled using a closed system of three Lytron heat exchangers mounted in the helicopter.

An optical system incorporating a reverse Cassegrainian telescope has been designed for focussing the laser beams. Passive and active methods have been described for controlling the focussing system. The former uses a focus analyzer similar to those found in commercial zoom lens while the latter has a laser range finder. The focussing system is capable of focussing the laser beams over a range of 20 to 30 m.

The laser beams are steered and kept on target by a large mirror mounted on a two-axis mount controlled by an infrared video tracker. The tracking system uses an infrared scanning radiometer to produce a television image of the laser-heated oil spot. This image is processed by a video tracker operating in the centroid mode to generate error signals proportional to the displacement of this spot from the center of the field of view. The error voltages are amplified to drive the biaxial mirror mount. In the prototype system the video tracker can be replaced by a human operator controlling a joystick.

An auxiliary power unit must be installed on the helicopter to satisfy the power requirements of the CW laser. The helicopter installation and configurational layout of the LIOS system and the APU are discussed. Costs, sizes, and weights of all system components are also identified.

REFERENCES

1. Lewis, E.L., "Oil in Sea Ice", (Unpublished Manuscript), Pacific Marine Science Report 76-12, Institute of Ocean Sciences, Victoria, B.C., June 1976.

2. Ross, S., "A Review of Countermeasures for a Major Oil Spill from a Vessel in Arctic Water", Submitted to Environment Canada, March 1982.

3. S. L. Ross Environmental Research Ltd., "Igniter Requirements for a Major Oil Spill from a Vessel in the Canadian Arctic", Environmental Emergencies Technology Division Report EE-56, Environment Canada, November 1984.

4. Frish, M.B., Simons, G.A., DeFaccio, M.A., and Nebolsine, P.E., "Laser Ignition of Oil Spills - Phase I: Concept Development", Physical Sciences Inc., TR-513, May 1985.

5. Nawwar, A.M., Frish, M.B., DeFaccio, M.A., Nebolsine, P.E., and Howard, D., "Laser Ignition of Oil Spills - Phase II: Outdoor Demonstration Experiments", Arctec Canada Ltd., Rept. 1758C-1, April 15, 1985.

6. Twaurdus, E.M., "A Study to Evaluate the Combustibility and Other Physical and Chemical Properties of Aged Oils and Emulsions", Environmental Emergencies Technology Division Report EE-5, Environment Canada, December 1980.

7. Wolfe, W.L. and Zissis, G.J., The Infrared Handbook, Environmental Research Institute of Michigan, 1978.

8. Fisher, D.W., Leftwich, R.F., and Yates, H.W., "Survey of Infrared Trackers", Applied Optics, Vol. 5, No. 4, 1966.

9. Snyder, W.J., Cross, J.L., and Schoultz, M.B.,"Vibration Investigation of a Large Transport Helicopter", Shock and Vibrations Bulletin, No. 47, Sept 1977.

10. Canadian Department of Transport Engineering and Inspection Manual, Parts 1 and 2, Canadian Government Publishing Center, Hull, Quebec, 1980.

TABLE 1

Item	Vendor	Model	Cost (Cdn)	Wt(lb)
REQUIRED OPTICS				
Breadboard	Newport Corp	XA Series	4800	200
Gimbal Mount	Aerotech	AOM 110-12	1440	40
Gimbal Mount	Aerotech	AOM 110-12	1440	40
10" Adaptor	Aerotech	AOM 1110	370	2
Parabolic Mirror	Edmund	F32,061	770	15
Flat Mirror	Custom		750	12
Ge Lens	Janos	A1301C323	600	.25
Ge Flat	Janos	A1305C652	525	.25
Mounting Rings	Custom		750	4
Translation Stage	Aerotech	ATS204	2660	11
Motorized Drive	Aerotech	1050DC/MO/ E500MB	1245	3
ZnSe Lens	Janos	Custom	900	.5
Miscellaneous			3000	5
			19,250	333
OPTION A - PASSIVE FOCUSSING				
Self-Focussing Module	?		2250	2
OPTION B - ACTIVE FOCUSSING				
Rangefinder	Optech	Model 60	18000	7.5
Motion Controller/ Computer Interface	Aerotech	UNIDEX II/SL/ 4020/DC-O/W	3975	30
Host Computer	Compaq		4500	20
Beam Combiner (replaces flat mirror)	CVI	Custom	750	0
			27,225	57.5
LASERS				
CW	LCA	Falcon 800	120,000	(Head) 308 (Console) 710
Pulsed	Lumonics	TEA-103-2	47,000	(Head) 375 (Control) 90
			167,000	1483

TABLE 1 (cont')

COOLING

Heat Exchangers	Lytron	6321 (x3)	1900	87
Pump	Teel	2P508	150	13
3/4 hp pump motor	Dayton	6K581	113	21
Hardware			375	10
			2,538	131

TABLE 2

Item	Vendor	Model	Cost (Cdn)	Weight (lb)
Targeting Mirror	Custom		1500	30
Mirror Mount	Custom		4000	50
Azimuth Stage	Micro-Controle	RT300	11000	40
Elevation Stage	Micro-Controle	BG200	12000	42
DC Motor/Encoder/ Tachometer	Aerotech	1135DC	4000	20
Joystick	Aerotech	JP	1100	0.5
Servo Amplifiers	Aerotech	100QV	1600	10
Power Supply/ Chassis	Aerotech		3100	30
DAC	Various		2000	2
Imaging IR Sensor	Inframetrics	525	46000	10
Video Tracker	DBA	606	45000	25
Video Camera	Various		2000	2
B/W Monitor	Inframetrics		2000	5
Computer	Compaq		4500	20
		Totals	139,800	287

TABLE 3

Item	Vendor	Model	Cost (Cdn)	Weight (lb)
APU	Turbomach	T-62T-16B1	100,000	100
Generator, fuel tank, fire extinguisher	Various		40,000	
Materials	Various		1,500	
Labor for installation			6,000	
			147,500	